INSTITUTO NACIONAL DE TECNICA AEROESPACIAL
"ESTEBAN TERRADAS"
Madrid, Spain

O P E N F I R E S
AND
T R A N S P O R T O F F I R E B R A N D S

Principal Investigator:
C. Sánchez Tarifa

Colaborators:
P. Pérez del Notario
A. Rodriguez Villa
A. Liñán Martinez
E. Mezquida

MAY 31, 1965 - MAY 31, 1966

INTRODUCTION

The research program on Open Fires and Transport of Firebrands conducted under Grant Fg-Sp-114 has been extended in order to complete and expand some parts of the research work and for the preparation of Final Report of Grant.

Therefore, the present document is the Fifth Annual Report of Grant Fg-Sp-114, which will be made concise since Final Report of Grant will be soon published. The research program on Open Fires has been devoted, mainly, to the theoretical and experimental studies on the scaling laws giving burning rates in pool fires as function of vessel diameter. The experimental investigation has been carried out by burning n-heptane and ethylene dioxide (dioxane) fuels.

On Transport of Firebrands the principal effort has been dedicated to the completion and final adjustment of the vertical variable cross-section wind tunnel in which combustion of firebrands is observed under free-flight conditions, as well as to carry out a research program in this wind tunnel.

In addition, the research work on combustion of wood with forced convection has been carried out in order to obtain dimensionless results and scaling laws; calculation of flight paths and burning out times from those data and statistycal studies on firebrands have been also continued.

- - - - - - - - -

I - OPEN FIRES

1 - INTRODUCTION

During the report period the research work on Open Fires has been devoted to the study of the influence of vesselsize on burning rates in the region of small diameters.

In Fourth Annual Report the value of burning rate as function of the physical properties of the fuel and of vessel diameter was shown in the region of large values of this diameter.

In this case, the radiation heat flux from flame to fuel is predominant and it controls the burning rate.

As vessel diameter decreases the burning rate also decreases, but it increases again when vessel diameter is very small. This fact has been experimentally confirmed [1,2,3] and several qualitative explanations of this phenomenon have been given.

During the present report period this phenomenon has been analyzed and a theoretical study of the process has been carried out. A mathematical expression for the burning rate has been derived which covers all field of variation of vessel diameters.

At the same time, an experimental investigation has been carried out, utilizing n-heptane and dioxane fuels.

2. THEORETICAL STUDIES

In small vessels the flame is small and, therefore, the radiant heat flux received by the fuel is also small. The increasement of burning rate observed experimentally in this region of small diameters must be due to the heat received by the fuel free surface from the flame through convection and owing to the heat transmitted through the vessel lateral walls. These two proces ses have been independently studied and they may be super-

imposed as a first approximation.

7.1 Heat Convection through the Free-Surface of the Fuel

Heat transfer from flame to the fuel surface takes place through convection, heat flux being in opposite direction to the fuel vapors flow.

For small vessels the flame is laminar and the volume occupied by the fuel vapors has an approximately conical shape, as it was pointed out in Third Annual Report.

It has been observed that, for laminar conditions, the height of the cone is of the same order of magnitude than that of the vessel radius.

Therefore, as a first approximation, both dimensions may be taken to be equal ($z_{v,max} = D/2$).

The heat received through convection, according to Eq. III-16(*), is

$$\dot{q}_{cf} = \lambda_v \frac{T_f - T_s}{z_v} \frac{\nu_v}{e^{\nu_v} - 1} = \frac{c_v \dot{m}_b' (T_f - T_s)}{e^{\nu_v} - 1} \qquad (1)$$

in which:

$$\nu_v = \frac{z_v c_v \dot{m}_b'}{\lambda_v} \qquad (2)$$

By taking as value of z_v a linear expression given by:

$$z_v = z_{v,min} \left[1 + \left(\frac{z_{v,max}}{z_{v,min}} - 1 \right) \left(1 - \frac{2r}{D} \right) \right] \qquad (3)$$

Eq. (3) gives the radial distribution of the heat received by the fuel surface through convection, which in turn, depends on

(*) Third Annual Report, Eq. 16.

the distribution of burning rate $\dot{m}_b$.

An approximation of the process, valid for small sized vessels, consists in disregarding radiation heat transfer to the fuel and in neglecting convective heat transfer within the fuel in a direction parallel to the fuel free surface.

These assumptions give the following equation for the balance of energy:

$$\dot{q}_{cf} = \dot{q}_{c\ell} + \dot{m}_b' \, q_\ell \qquad (4)$$

From this equation and taking into account equations (1) and (3)*, when $\nu_\ell >> 1$, which is the normal case, it is obtained·

$$\frac{\dot{m}_b' \, c_v \, (T_f - T_s)}{e^{\nu_v} - 1} = \dot{m}_b'' \left[q_\ell + c_\ell \, (T_s - T_o) \right] \qquad (5)$$

from which, it results:

$$\dot{m}_b' = \frac{\lambda_v}{c_v \, z_v} \ln \left[1 + \frac{c_v \, (T_f - T_s)}{q_\ell + c_\ell \, (T_s - T_o)} \right] \qquad (6)$$

which gives the burning rate distribution as function of z_v , or with equation (6) as function of radius.

Burning rates ratios, taking into account (6), are:

$$\frac{\dot{m}_b''}{\dot{m}_{bo}''} = \frac{1}{1 + \left(\frac{z_{v,max}}{z_{v,min}} - 1 \right) \left(1 - \frac{2r}{D} \right)} \qquad (7)$$

This expression is shown in Fig.10, in which the influence of vessel diameter may be observed.

---

* Third Annual Report.

Radiant heat flux and possible heat transfer within the liquid could make less sharp the burning rate curve.

The average value of burning rate is given by:

$$\dot{m}_b = \frac{4}{\pi D^2} \int_0^{D/2} \dot{m}_b' 2\pi r dr \Big/ \frac{2\lambda_v}{c_v} \ln \left[1 + \frac{c_v (T_f - T_s)}{q_{\ell_c} + c_\ell (T_s - T_o)} \right] \times$$

$$\times \int_0^1 \frac{1}{z_v} \frac{2r}{D} d\frac{2r}{D}$$

and considering equations (*) and ( ), it results:

$$\dot{m}_b = \frac{\lambda_v}{c_v z_{v,min}} \ln \left[1 + \frac{c_v (T_f - T_s)}{q_\ell + c_\ell (T_s - T_o)} \right] \frac{2}{(\beta-1)^2} (\beta \ln\beta - \beta + 1) *$$

$$= \dot{m}_{bo}' \frac{2}{(\beta - 1)^2} (\beta \ln\beta - \beta + 1)$$

in which:

$$\beta = \frac{z_{v,max}}{z_{v,min}}$$

Fig.2 shows the value of $\dot{m}_b / \dot{m}_{bo}'$ assuming $z_{v,max} = D/2$. It may be seen that mean burning rate decreases when the vessel diameter augments.

Considering that the influence of radiation is small for small vessel diameters and that, on the other hand, convection is negligeable for large diameters, both effects can be superimposed. Then, equations (8) and (IV-I.7) * give the expression of burning rate valid for all range of diameters, that is:

* Fourth Annual Report.

$$\dot{m}_b = \frac{\lambda_v}{c_v\, z_{v,min}} \ln \left[1 + \frac{c_v\,(T_f - T_s)}{q_\ell + c_\ell (T_s - T_o)} \right] \frac{2}{\left(\frac{D}{2 z_{v,min}} - 1 \right)^2} \times$$

$$\times \left[\frac{D}{2\, z_{v,min}} \ln \frac{D}{2\, z_{v,min}} - \frac{D}{2\, z_{v,min}} + 1 \right] +$$

$$+ \frac{\sigma T_f^4}{q_\ell + c_\ell\,(T_s - T_o)} \left[1 - \exp \left(-0{,}0055\ \alpha \frac{q_r}{q_\ell} D \right) \right] \qquad (9)$$

Fig.3 shows results obtained for n-heptane and dioxane fuels. It may be observed the similarity of these results with those experimentally obtained by several investigators.

7.2 Convection Through the Lateral Walls of Vessel

Heat exchange between the liquid fuel and vessel wall can be of certain importance, depending on the degree of cooling of the vessel. Through that wall, the fuel can receive heat from the flame or by the contrary, it may give off heat to the cooling fluid.

The expression of the heat transferred from the wall is:

$$\dot{Q}_w = \pi D x_s h\, (T_w - T_{fm}) \qquad (10)$$

in which T_w and T_{fm} are the average temperatures of wall and fuel, and h is the convective heat transfer coefficient. For this coefficient the following expression may be taken:

$$Nu = \frac{hD}{\lambda} = A \left(\frac{m_b D}{\mu} \right)^a \left(\frac{\mu c_p}{\lambda} \right)^b \left(\frac{D}{x_s} \right)^c \qquad (11)$$

No complete information exists on the experimental values of

coefficients A , a , b , and c for a wide range of variation of D/x_s . When $D/x_s >> 1$ the influence of heat exchange through the wall is small as compared with the other heat transfer mechanism and then it may be disregarded. On the other hand, when $D/x_s < 1$, the existing experimental data for tubes may be utilized as a first approximation, and this approximation improves as the ratio D/x_s becomes smaller, which is the case being studied.

Fuel motion in the vessel is laminar, and then, the following expression may be utilized:

$$Nu = \frac{hD}{\lambda} = 1{,}86 \left(\frac{\dot{m}_b D}{\mu}\right)^{1/3} \left(\frac{\mu c_p}{\lambda}\right)^{1/3} (D/x_s)^{1/3} \qquad (12)$$

in which fuel properties must be referred to the average temperature $T_m = (T_o + T_s)/2$.

Under these assumptions, the heat received by the fuel from the wall through convection, per unit area of free surface, and for a circular vessel, is given by

$$\dot{q}_w = \frac{4\,\dot{Q}_w}{\pi D^2} = 4 \cdot 1{,}86 \lambda \left(\frac{c_p}{\lambda}\right)^{1/3} \dot{m}_b^{1/3} D^{-4/3} x_s^{2/3} \cdot (T_w - T_m) \qquad (13)$$

in which equations (10) and (12) have been taken into account.

Considering this heat exchange, for small values of D that is, when radiation is small, the equation expressing the energy balance is:

$$\dot{q}_w + \dot{q}_{cp} = \dot{m}_b \left[q_\ell + c_s (T_s - T_o) \right] \qquad (14)$$

The left hand side of this expression implicitly contains burning rate $\dot{m}_b$, and its determination from that equation is difficult. A first approximation is to assume that no interaction exists between the direct convection flame-fuel and the indirect

one through the wall, and then to superimpose both effects, that is to say:

$$\dot{m}_b = (\dot{m}_b)_{\dot{q}_w=o} + (\dot{m}_b)_{\dot{q}_{cf}=o} \qquad (15)$$

In this expression $(\dot{m})_{\dot{q}_w=o}$ is given by (8) and $(\dot{m}_b)_{\dot{q}_{cf}=o}$ is derived from (13), being:

$$(\dot{m}_b)_{\dot{q}_{cf}=o} = \left[\frac{7{,}44\ \lambda\ (c_p/\lambda)^{1/3} (T_w - T_m)^{1/3}\ D^{-4/3}}{q_\ell + c_\ell\ (T_s - T_o)} \right]^{3/2} \qquad (16)$$

Fig. 11 shows the results obtained from this expression for n-heptane.

Actually, the convective effect from the wall should be in some degree larger than that given by (16), since $\dot{m}_b > (\dot{m}_b)_{\dot{q}_{cf}=o}$ and the convective effect on the fuel surface should be somewhat smaller than that given by (8), since $\dot{m}_b > (\dot{m}_b)_{\dot{q}_w=o}$.

It may be pointed out that the convective effect from the wall can be positive or negative according to the sign of ΔT .

Superimposing all these effects, the general expression giving explicitly the burning rate is:

. . . . / . . .

$$\dot{m}_b = \frac{\lambda_v}{c_v\, z_{v,min}} \ln\left[1 + \frac{c_v\,(T_f - T_s)}{q_\ell + c_\ell\,(T_s - T_o)}\right] \frac{2}{\left(\frac{D}{2\, z_{v,min}} - 1\right)^2} \times$$

$$\times \left[\frac{D}{2\, z_{v,min}} \ln \frac{D}{2\, z_{v,min}} - \frac{D}{2\, z_{v,min}} + 1\right] +$$

$$+ \left[\frac{7{,}44\,\left(\frac{c_p}{\lambda}\right)^{1/3} \Delta T D^{-4/3}}{q_\ell + c_\ell\,(T_s - T_o)}\right]^{3/2} + \frac{\sigma T_f^4}{q_\ell + c_\ell\,(T_s - T_o)}\left[1 - \exp(-0{,}0055\alpha\, \frac{q_r}{q_\ell}\, D)\right]$$

(17)

in which:

$$\Delta T = T_w - \frac{T_s + T_o}{2}$$

In Fig.5 results obtained from this expression are represented for a particular case.

3. EXPERIMENTAL RESULTS

The experimental work has been devoted to the study of the radial distribution of the burning rate and to the measurement of $\dot{m}_b$ for small vessels.

To accomplish this program, the research facility was modified as shown in Figs. 6 and 7, utilizing two vessels of 250 mm and 72 mm in diameter divided in three annular compartments of equal area.

In Figs. 27 and 28 some of the experimental results obtained are shown. Each point represents the average value of at least ten measurements.

In Fig. 27 it may be observed that $\dot{m}_b$ increases from the center of the vessel to the rim, when vessel cooling is poor, result which is in agreement with the theoretical prediction (Fig. 11)

It may also be observed that burning rate decreases noticeably near the rim when vessel cooling is increased. Therefore, for small vessels, the convective heat flux from the vessel wall, either positive or negative, exerts an important influence on the value of the burning rate $\dot{m}_b$

According to this, it may be concluded that the increasement of burning rate as vessel diameter is reduced, as stated by several investigators[1,2,3], depends, largely on the experimental technique that has been selected.

When combustion takes place in only one of the annular compartment of the vessel of 72 mm in diameter either at the central or at the intermedial one, combustion rate is higher. This is due to heat transferred from the walls, since in this case this convection effect from the walls is more important than in the case of the vessel being completely filled with fuel.

When combustion takes place at the outer compartment combustion rate is lower because its outer wall is cooled.

For the large vessel (Fig.9) the distribution of $\dot{m}_b$ is similar when dioxane fuel is utilized. On the other hand, when n-heptane is burned the distribution of $\dot{m}_b$ changes, being almost constant due to the more important influence of radiation of the n-heptane as compared with the dioxane flame.

Finally, it may pointed out that all experimental results agree very well with those predicted theoretically as it may be seen by comparing the results shown in Figs. 1, 4, 5, 8 and 9

II - TRANSPORT OF FIREBRANDS

1 INTRODUCTION

During the report period the research program on transport of firebrands has comprised the following subjects:

a) Completion and final adjustment of the vertical wind tunnel of variable cross-section area to study combustion of firebrands under free-flight conditions.

b) Determination of terminal velocities of fall as function of time and burning-out times by using the vertical free-flight tunnel.

c) Continuation of the measurements on combustion of wood particles with forced convection at constant wind speed, in order to calculate terminal velocities of fall and burning-out times under actual flight conditions.

d) Dimensional analysis of theoretical and experimental results of combustion of firebrands at constant wind speed and at wind speed equal to final velocity of fall.

e) Continuation of some studies on statistical behaviour of firebrands.

2 VERTICAL FREE-FLIGHT WIND TUNNEL

The vertical wind tunnel, designed to study combustion laws of firebrands under free-flight conditions has been completed and utilized. It has proved to be a very valuable and extremely simple research facility, specially suitable for determining burning-out times of firebrands.

A drawing of this tunnel was included in Fourth Annual Report and a photograph of it is shown in Fig.10.

The wind tunnel consists of a cone of 3000 mm in length

manufactured of transparent plastic material. On top of the cone a cylindrical section of 1400 mm in length is attached, on which another smaller cone is placed supporting the suction blower.

The wind tunnel is calibrated by introducing in it several wood spheres of different size. Their terminal velocities of fall are known, and the spheres become distributed along the cone according to size, giving an indication of the average value of the air velocity at each location.

When a firebrand is introduced through the lower intake it climbs up as it burns, and its terminal velocity of fall is recorded by comparison with that of the sphere with the same average location or by taking photographs.

At first, the wind tunnel had a high degree of vorticity and the firebrands had a strong tumbling motion. This effect has been reduced down to tolerable limits after several modifications.

By taking long exposure time photographs, the effect of tumbling can be avoided, since these photographs give the average location of firebrands as function of time

In this way it is possible to measure terminal velocities of fall and results agree well with those obtained with the vertical or horizontal wind tunnels in which the firebrands were kept attached at a fixed position. An example of this is shown in Fig.11.

However, with this wind tunnel measurements of terminal velocities of fall are lengthy and somewhat difficult due of the unavoidable tumbling motion of firebrands. On the other hand, the tunnel is extremely useful for measuring burning-out times of firebrands, which is the most important parameter in the aerodynamic behaviour of firebrands. Measurements consist simply in checking the elapsed time since the firebrand is introduced through the lower intake till it is consumed, usually

at the cylindrical section in which air speed is very low.

A series of systematic measurements are being carried out to determine burning-out times of spherical, cylindrical and plate-shaped firebrands, and some of them are shown in Figs.12, 13, 14 and 15 which are summarized in Figs. 16 and 17.

3 COMBUSTION OF WOOD WITH FORCED CONVECTION

The studies on combustion of wood particles with forced convection, that is, when air at constant velocity is blowing over the firebrand, have been continued.

The scope of these studies is the attainment of basic laws on combustion of wood and determination from these data of flight paths of firebrands.

Is has been shown in the preceding Reports[1,2,3,4] that firebrands fly at a velocity which is practically equal to the final velocity of fall and that this velocity reduces as the firebrands burns. Therefore, under actual flight conditions combustion of firebrands occurs at variable wind speed.

Research facilities[1,2,3] have been built to study combustion of firebrands when exposed to a wind blowing at a velocity constantly equal to the firebrand final velocity of fall.

However, the main objective of the aforementioned study is to investigate the possibility of determining flight paths of firebrands from the experimental results obtained when the firebrands are burnt at constant air speed, since research facilities are simpler and conclusions are more general when they are obtained from basic laws on wood combustion.

In order to carry out this program, the principal variables of a firebrand, such as mass, volume, density and aerodynamic drag are being determined as function of time for several wind speeds.

Functions:

$$m = f_1 (w, t) \qquad (20)$$

$$V = f_2 (w, t) \qquad (21)$$

$$\rho_w = f_3 (w, t) \qquad (22)$$

$$D = f_4 (w, t) \qquad (23)$$

are being experimentally obtained for spheres, cylinders and plates of pine, aspen, oak and balsa wood.

Some of those results have been already shown in Fourth Annual Report, and in Figs. 17 through 22 some of the results which are presently being obtained are shown.

From these functions, final velocities of fall,

$$w_f^c = \frac{mg}{\frac{1}{2} \rho_a C_D S} = f_5 (w, t) \qquad (24)$$

are immediately determined (*).

4 DIMENSIONAL ANALYSIS

Theoretical and experimental results will be expressed in dimensionless form. In the first place, this study will be applied to the case of combustion of wood with forced convection at constant wind speed.

A firebrand will be characterized by its initial density $\rho_{w,o}$ and by three characteristic lengths D_o, L_o, and l_o. On the other hand, air will be characterized by its density ρ_a and viscosity μ_a.

(*) NOTE.- Superscript c will be used to denote final velocities of fall of firebrands burning at constant wind speed.

According to dimensional analysis, any property ξ of the firebrand referred to its initial value ξ_o, will be given by an expression of the form:

$$\frac{\xi}{\xi_o} = \Phi \left[\left(\frac{wt}{D_o}\right)^{\alpha}, \left(\frac{wD_o\rho_a}{\mu_a}\right)^{\beta}, \left(\frac{\rho_{w,o}}{\rho_a}\right)^{\gamma}, \left(\frac{L_o}{D_o}\right)^{\delta}, \left(\frac{l_o}{L_o}\right)^{\varepsilon} \right] \quad (25)$$

or:

$$\frac{\xi}{\xi_o} = \Phi \left[\chi^{\alpha}, Re^{\gamma}, \zeta^{\gamma}, \lambda_1^{\delta}, \lambda_2^{\varepsilon} \right] \quad (26)$$

In this expression, $\chi = wt/D_o$ is a characteristics parameter of this non-stationary combustion; $Re = wD_o\rho_a/\mu_a$ is the Reynolds number; $\zeta = \rho_{w,o}/\rho_a$ is a parameter characterizing the kind of wood, and parameters $\lambda_1 = L_o/D_o$ and $\lambda_2 = l_o/L_o$ represent the firebrand's shape.

For cylindrical firebrands, we have:

$$\frac{\xi}{\xi_o} = \Phi \left[\chi^{\alpha}, Re^{\beta}, \zeta^{\gamma}, \lambda_1^{\delta} \right] \quad (27)$$

and for spherical firebrands:

$$\frac{\xi}{\xi_o} = \Phi \left[\chi^{\alpha}, Re^{\beta}, \xi^{\gamma} \right] \quad (28)$$

If results are restricted to only one kind of wood they will be simply expressed in the form:

$$\frac{\xi}{\xi_o} = \Phi \left(\chi^{\alpha}, Re^{\beta} \right) \quad (29)$$

Variable ξ can be the mass, volume, density, aerodynamic drag of the firebrand or final velocity of fall. In particular, burning-out time t_b of a firebrand will be expressed in the form:

$$\frac{wt_b}{D_o} = \chi_{t=t_b} = F\left[Re^{\alpha}, \xi^{\beta}\right] \quad \text{(spheres)} \qquad (30)$$

All results obtained for combustion of wood with forced convection are being expressed in this way. Fig.23 shows results obtained for spherical and cylindrical firebrand of oak wood with convection velocities ranging from 4 to 14 m/sec. All results have been correlated by means of the expressions:

$$\frac{w_f^c}{w_{f,o}} = F(U) \qquad (31)$$

being:

$$U = \frac{wt}{D_o} \times \left(\frac{wD_o\rho_a}{\mu_a}\right)^{-0.4} \qquad (32)$$

for spheres, and:

$$U = \frac{wt}{D_o} \times \left(\frac{wD_o\rho_a}{\mu_a}\right)^{-0.4} \times \left(\frac{L_o}{D_o}\right)^{-0.4} \qquad (33)$$

for cylinders.

It may be seen that the correlation is excellent. Considering that each experimental curve $w_f^c/w_{f,o} = f(U)$ is the average value of 5-6 experiments, in Fig.23 are represented a total of 126 experiments, which gives a good example of the very important saving in time and space resulting from this dimensionless presentation of results.

5.1 FINAL VELOCITIES OF FALL

Under actual flight and burning conditions, mass, aerodynamic drag, density, etc. of a firebrand have a functional dependency on time, since they depend on the complete time-history of the wind velocity and then, on the complete combustion process.

This functional dependency implies that in order to calculate actual flight paths of firebrands when flying and

burning at their final velocity of fall, starting from combustion data obtained at constant wind speed, a complementary assumption has to be introduced.

This complementary assumption is needed because the complete basic laws of wood combustion under non-stationary conditions are not known, this lack of knowledge being mostly due to the heterogeneous properties of wood.

A reasonable assumption which gives a very good approximation in practice is to assume that the elementary variation of the final velocity of fall w_f of the firebrand when it burns at the final velocity of fall, is equal to the elementary variation of final velocity w_f^c when the firebrand burns at constant wind speed w, when this velocity is equal to w_f. That is:

$$\frac{dw_f}{dt} = \left(\frac{dw_f^c}{dt}\right)_{w=w_f} \qquad (34)$$

Therefore, once an analytical expression is found for function:

$$\frac{w_f^c}{w_{f,o}} = F\,(\chi\ ,\ Re\ ,\ \xi\ ,\ \lambda_1\ ,\ \lambda_2) \qquad (35)$$

the expression of w_f as function of time is obtained by integrating the differential equation:

$$\frac{d}{dt}\left(\frac{w_f}{w_{f,o}}\right) = (F_\chi)_{w=w_f} \times \frac{d\chi}{dt} \qquad (36)$$

The resulting analytical expression of w_f will be compared with the experimental results directly obtained.

A similar method was followed in ref.[5] to obtain final velocities of fall, but starting from the value of the firebrand radius when burning at constant wind speed.

5.2 COMPARISON OF RESULTS

Experimental results obtained when the firebrands burn at wind speeds constantly equal to the final velocities of fall are being represented in dimensionless form. Any firebrand property η, such as weight, density, diameter, aerodynamic drag and final velocity of fall, will be expressed in the form:

$$\frac{\eta}{\eta_o} = \Phi \left[\chi_f^{\alpha} , \; Re_f^{\beta} , \; \zeta^{\gamma} , \; \lambda_1^{\delta} , \; \lambda_2^{\epsilon} \right]$$

in which ζ, λ_1 and λ_2 were defined in expressions (29), (30) and (31) and χ_f and R_{ef} are:

$$\chi_f = \frac{w_{f,o}\, t}{D_o} \tag{38}$$

$$R_{ef} = \frac{w_{f,o}\, D_o\, \rho_a}{\mu_a} \tag{39}$$

In particular, final velocities of fall of spherical and cylindrical firebrands of oak wood were represented with the expression:(*)

$$\frac{w_f}{w_{f,o}} = \Phi \left[\frac{w_{f,o}\, t}{D_o} \times \left(\frac{w_{f,o}\, D_o \rho_a}{\mu_a} \right)^{-0.4} \times \left(\frac{L_o}{D_o} \right)^{-0.4} \right] \tag{40}$$

or:

$$\frac{w_f}{w_{f,o}} = \Phi \, (Z) \tag{41}$$

(*) The experimental fact that exponents of dimensionless variables χ and χ_f, Re and R_{ef} and ξ, λ_1 and λ_2 are equal in expressions (40) and (33) is consistent with the analytical transformation (36) which gives the analytical expression of (40) starting from (26).

Results corresponding to 32 experiments are shown in Fig.24. It may be seen that the correlation of results is very good.

Finally, experimental values of $w_f^c/w_{f,o} = F(U)$ of Fig.23 were approximated by means of a curve defined with an initial parabolic expression followed by a straight line, as shown in Fig.25. Then, by means of (36) the analytical expression of $w_f = f(t)$ was obtained and represented in Fig.25. It can be seen that this curve agrees very well with the experimental curve.

This shows the feasibility of deriving actual results $w_f = f(t)$ when the firebrand flies at its final velocity of fall starting from experimental data obtained by burning firebrands at constant wind speed.

These studies are presently being extended to other kind woods with similar conclusions, and they will be shown in full in Final Report.

6. STATISTICAL STUDIES ON FIREBRANDS

These studies on firebrands are needed because of the statistical nature of the distribution according to size and shape of firebrands within a certain forest area, and because firebrands do not leave the convection column at prescribed points, but they are thrown away at random because of the strong turbulence that always exists within a well developed convection column.

Therefore, the point at which a firebrand leaves the convection column depends on a probability function which in turn has to be a function of both height and initial position of the firebrand with respect to the boundaries of the convection column. These studies are still in a preliminary phase, and some results already obtained were shown in Research Progress Report No. 9.

C O N C L U S I O N S

The principal finding and conclusions obtained during the report period are the following:

O P E N F I R E S

1) An analytical expression giving burning rate distribution as function of vessel radius has been obtained.

2) An analytical expression for the over-all burning rate as function of the physical properties of fuel (c_v , λ , q_l , T_s , q_r), as well as function of both flame radiant properties (α, T_f) and vessel diameter has been derived.

3) The influence of the lateral walls of vessel on burning rate has been obtained analytically.

4) For small vessel diameters it has been found that the influence of lateral walls on burning rate is very important.

F I R E B R A N D S

5) Vertical wind tunnels of variable cross-section area can be utilized to study combustion of firebrands under actual flight conditions.

6) From combustion of firebrands at constant wind speed it is possible to derive accurately results corresponding to actual flight conditions.

7) All results on combustion of firebrands can be expressed in dimensionless form using five parameters.

8) Parameters are the Reynolds number, densities ratio $\rho_w/\rho_{w,o}$, the ratio of two characteristic lengths to another one and parameter wt/D_o characteristics of non-stationary combustion processes.

- - - - - - - -

R E F E R E N C E S

1. SANCHEZ TARIFA, C.- et al : OPEN FIRES AND TRANSPORT OF FIRE BRANDS. First Annual Report. INTA, Madrid, 1962.

2. SANCHEZ TARIFA, C.- et al : OPEN FIRES AND TRANSPORT OF FIRE BRANDS. Second Annual Report. INTA, Madrid, 1963.

3. SANCHEZ TARIFA, C.- et al : OPEN FIRES AND TRANSPORT OF FIRE BRANDS. Third Annual Report. INTA Madrid 1964.

4. SANCHEZ TARIFA, C.- et al : OPEN FIRES AND TRANSPORT OF FIRE BRANDS. Fourth Annual Report. INTA Madrid 1965.

5. SANCHEZ TARIFA, C, P. PEREZ DEL NOTARIO and F. GARCIA MORENO : ON THE FLIGHT PATHS AND LIFE-TIMES OF BURNING PARTICLES OF WOOD. Tenth Symposium (International) on Combustion, 1965.

- - - - - - - -

NOTATION

I. O P E N F I R E S

c . . Specific heat at constant pressure

c_l . . Specific heat of the liquid fuel

c_v . . Specific heat of the vapor fuel

D . . Diameter of the burner

h . . Convective heat transfer coefficient

$\dot{m}$ . . Fuel flow within the vessel

$\dot{m}_b$ . . Local value of burning rate as function of radius

$\dot{m}'_{bo}$ . . Local value of burning rate, at vessel's center

Nu . . Nusselt number

$\dot{q}_{cl}$ . . Heat transferred through conduction throughout the liquid per unit area and per unit time.

$\dot{q}_{cf}$ . . Heat transferred through conduction to the surface per unit area and per unit time.

q_l . . Latent heat of evaporation

q_r . . Heat of reaction.

$\dot{q}_w$ . . Heat transferred to the fuel from the wall

r . . Radius of the burner

T_f . . Flame temperature

T_o . . Initial fuel temperature

T_s . . Surface temperature

T_w . . Average temperature of wall

x_s . . Vessel (fuel) depth

Z_v . . Vertical coordinate in the vapor zone, (Third Annual Report)

α . . Emission coefficient

λ . . Thermal conductivity

μ . . Liquid viscosity

ν . . Dimensionless parameter defined by (2)

σ . . Stefan-Boltzmann constant

II. TRANSPORT OF FIREBRANDS

D . . Aerodynamic drag of firebrand

g . . Acceleration of gravity

m . . mass of firebrand

t . . time

t_b . . burning out time

Re . . Reynold's number

V . . Volume of firebrand

w . . Relative wind speed

w_f . . Final velocity of fall of the firebrand

U, Z . Dimensionless variables

ρ_a . . Air density

μ_a . . Air viscosity

ρ_w . . Density of firebrand

λ_1, λ_2. Ratio of characteristic lengths.

$\xi, \eta, \alpha, \rho, \gamma, \epsilon, \delta$ - Parameters and variables

o . . Subscript denoting initial conditions

c . . Superscript denoting final velocities of fall of a firebrand burning at constant wind speed.

$\chi = wt/D_o$ Dimensionlees variable

ζ . . Ratio of densities.

- - - - - - - - -

FIG. 1

RADIAL DISTRIBUTION OF BURNING RATE

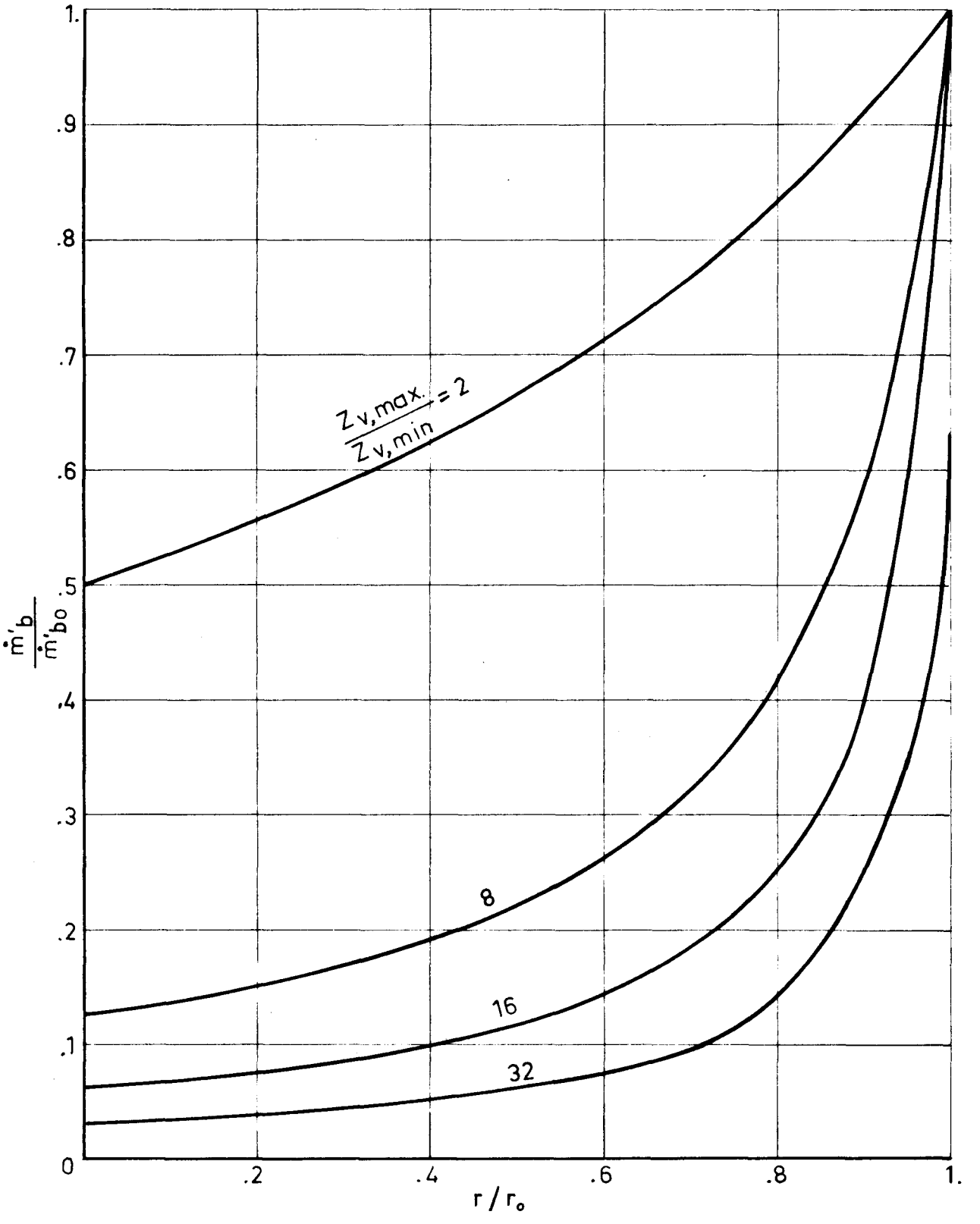

FIG. 2

INFLUENCE OF FUEL FREE SURFACE CONVECTION

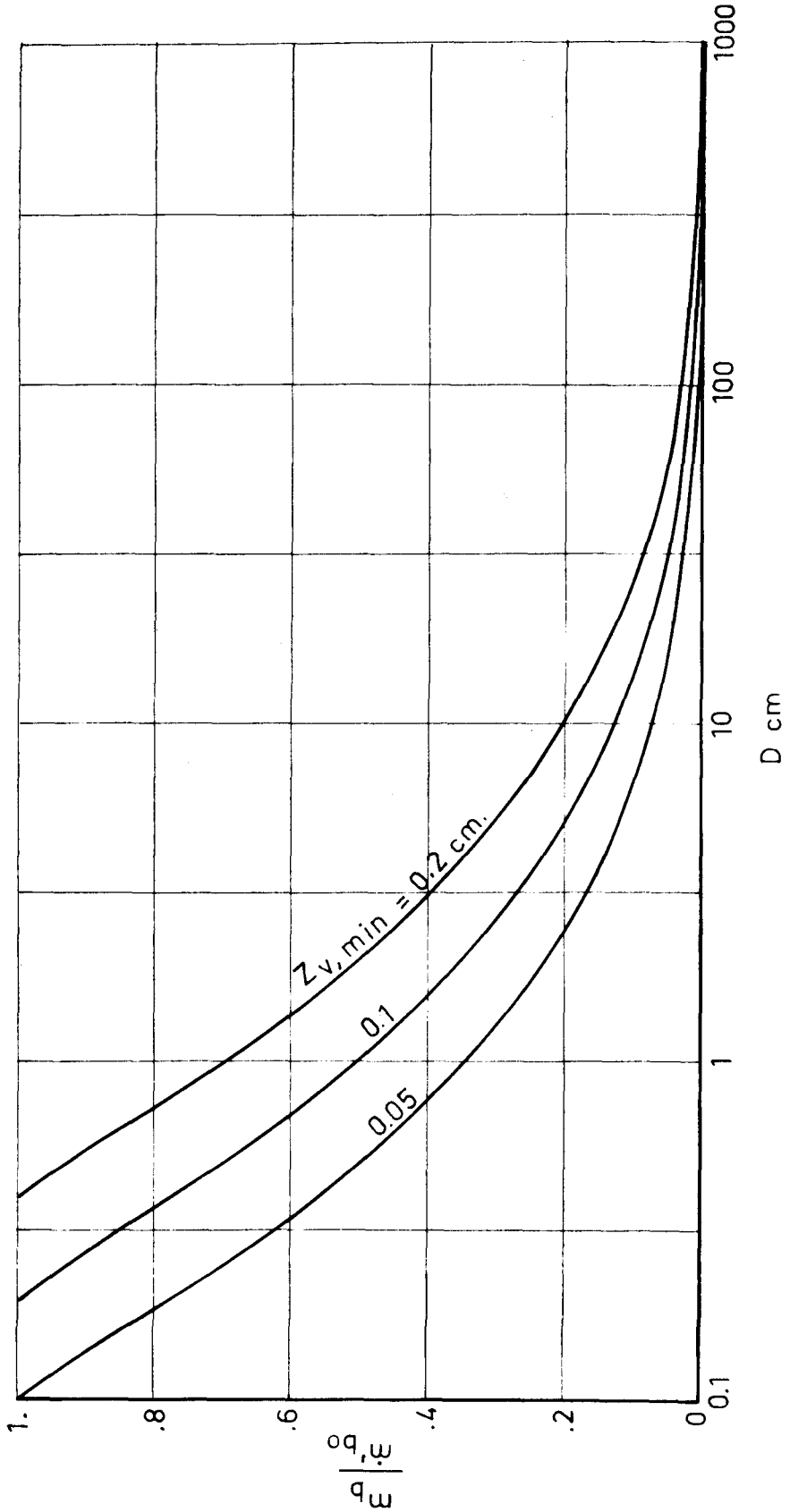

VARIATION OF BURNING RATE
(Only considering radiation and free surface convection)

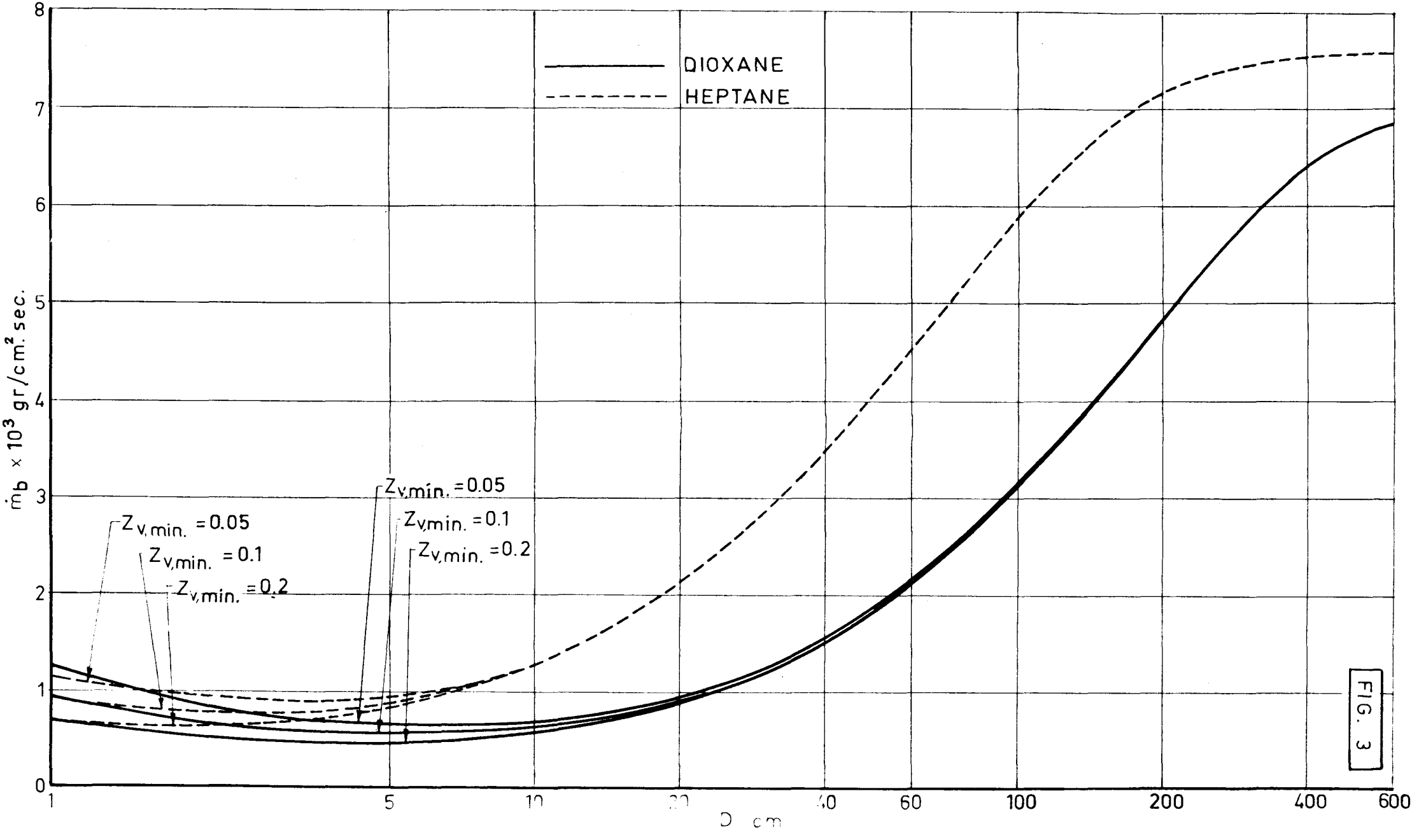

FIG. 3

FIG. 4

INFLUENCE OF WALL CONVECTION

HEPTANE

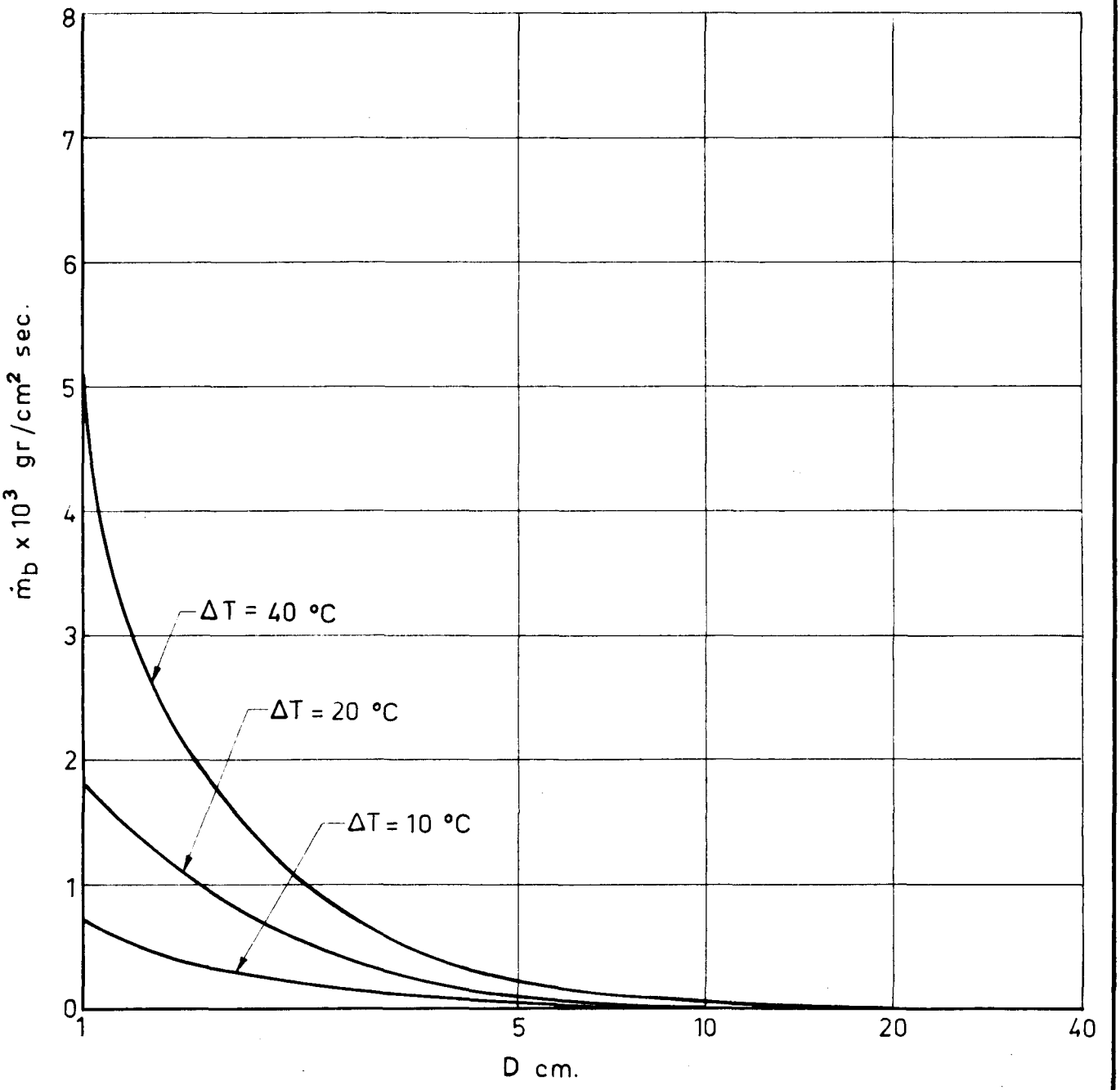

GENERAL EXPRESSION OF BURNING RATE VERSUS DIAMETER

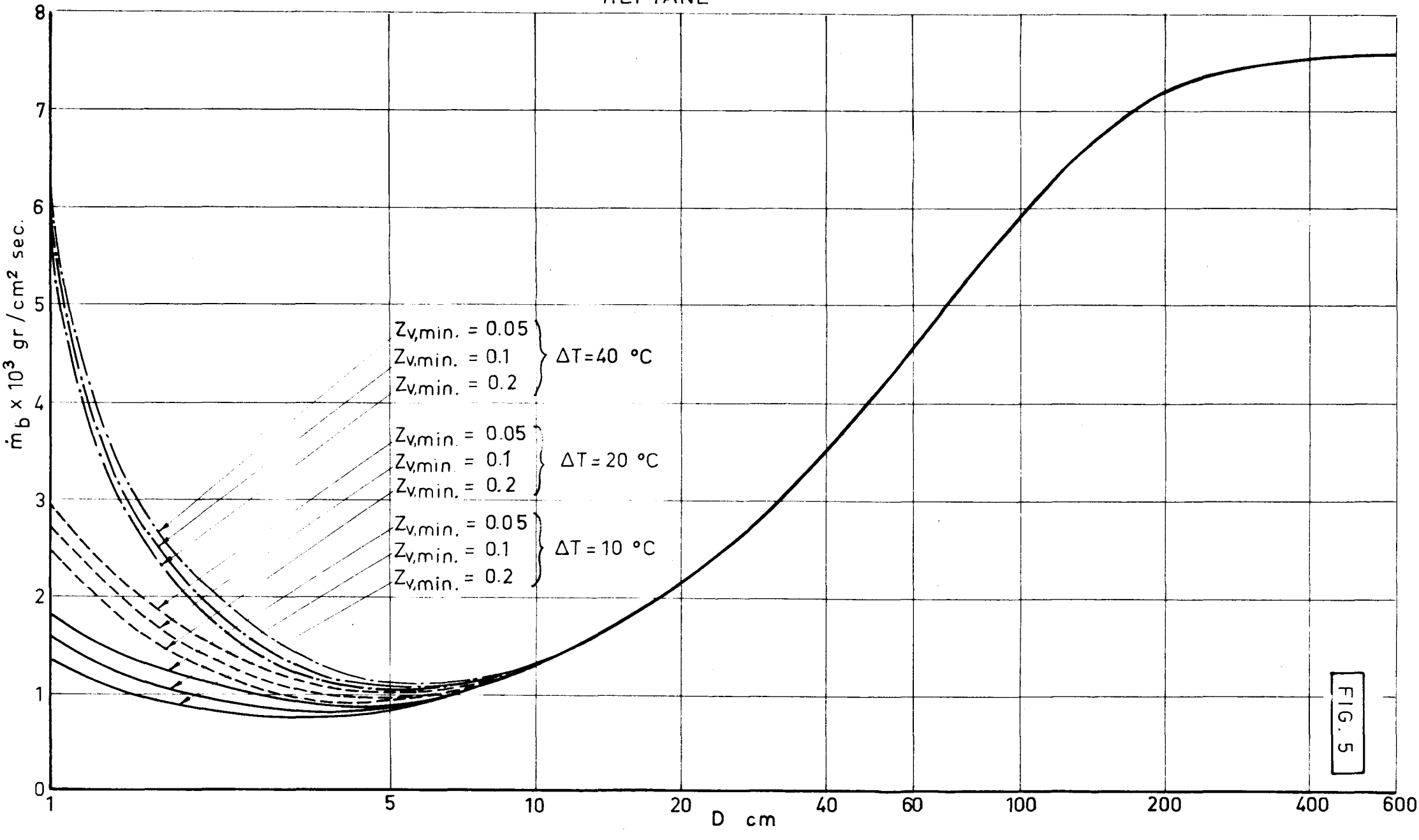

FIG. 5

SCHEMATIC DIAGRAM OF THE RESEARCH FACILITY

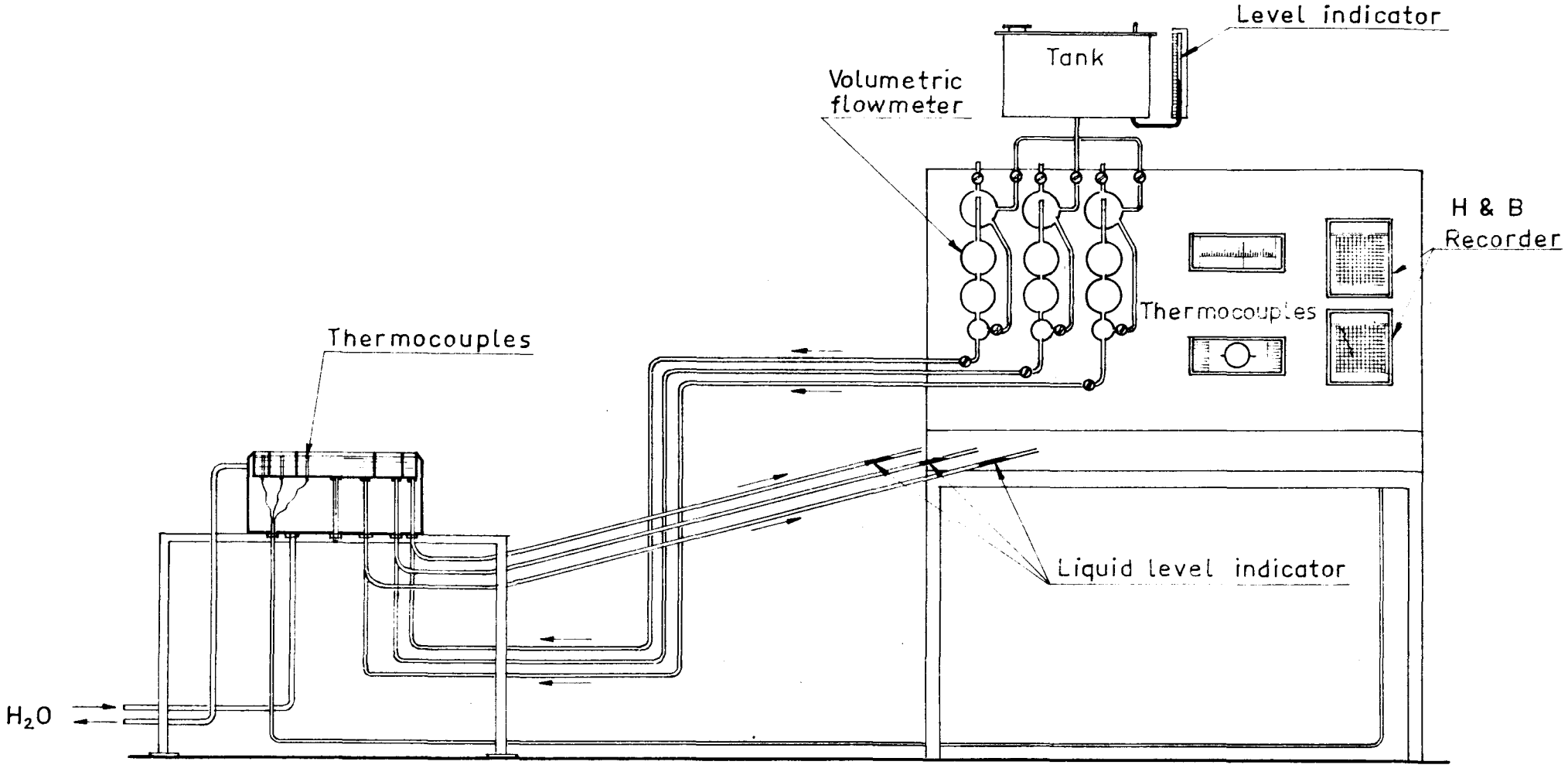

Fig. 6

VESSELS

FIG. 7

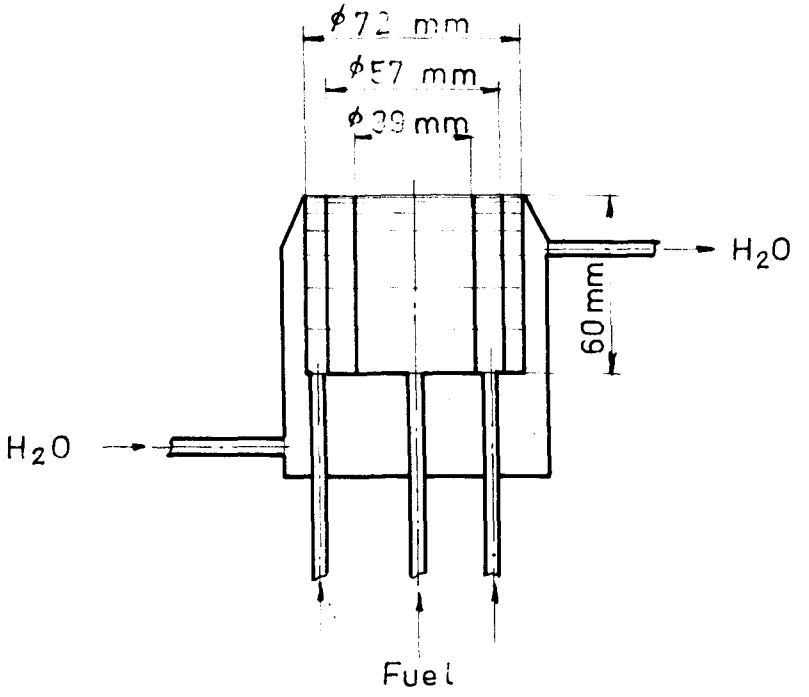

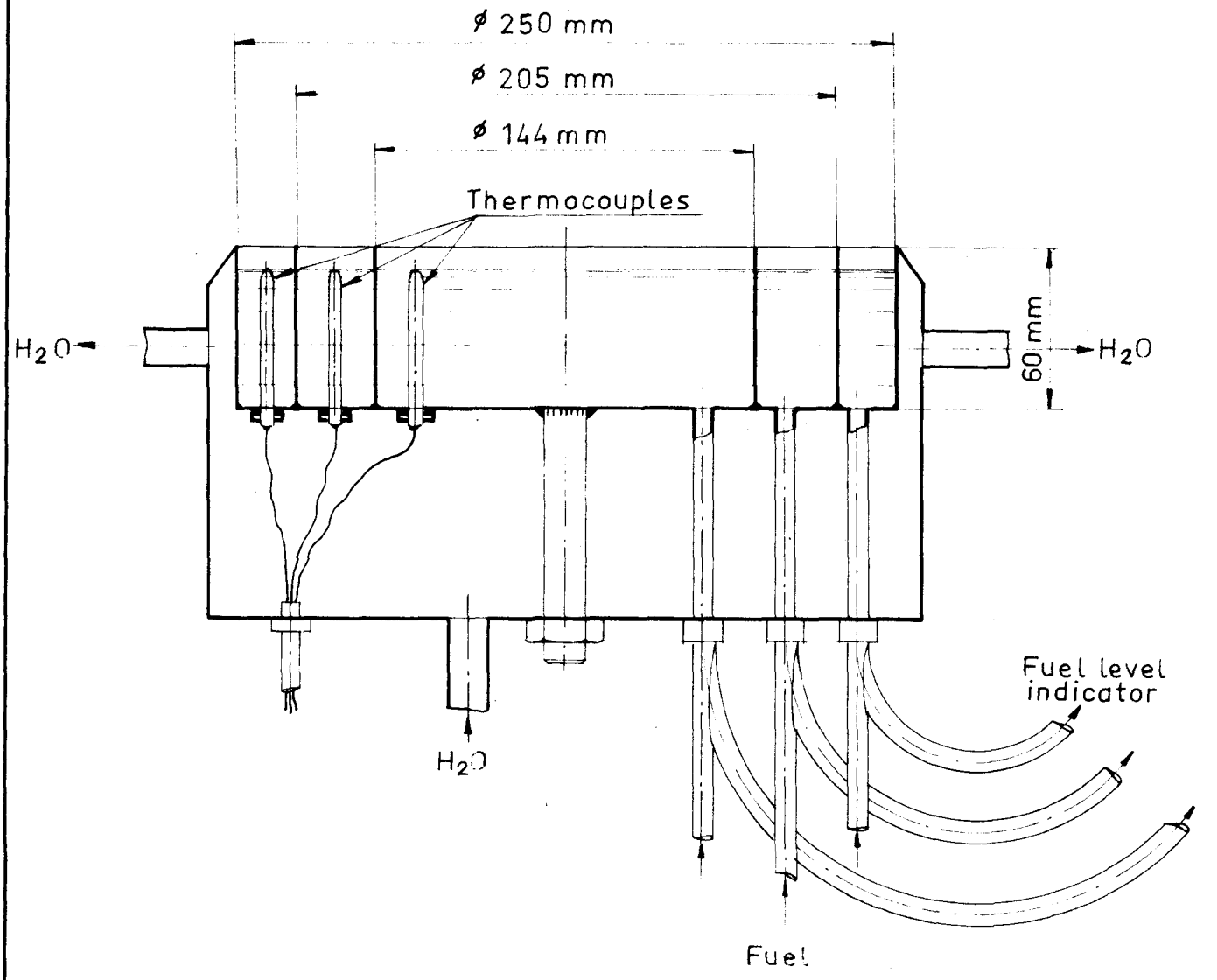

EXPERIMENTAL RESULTS

FIG. 8

HEPTANE

Vessel ∅ 40, 58, 72 mm.

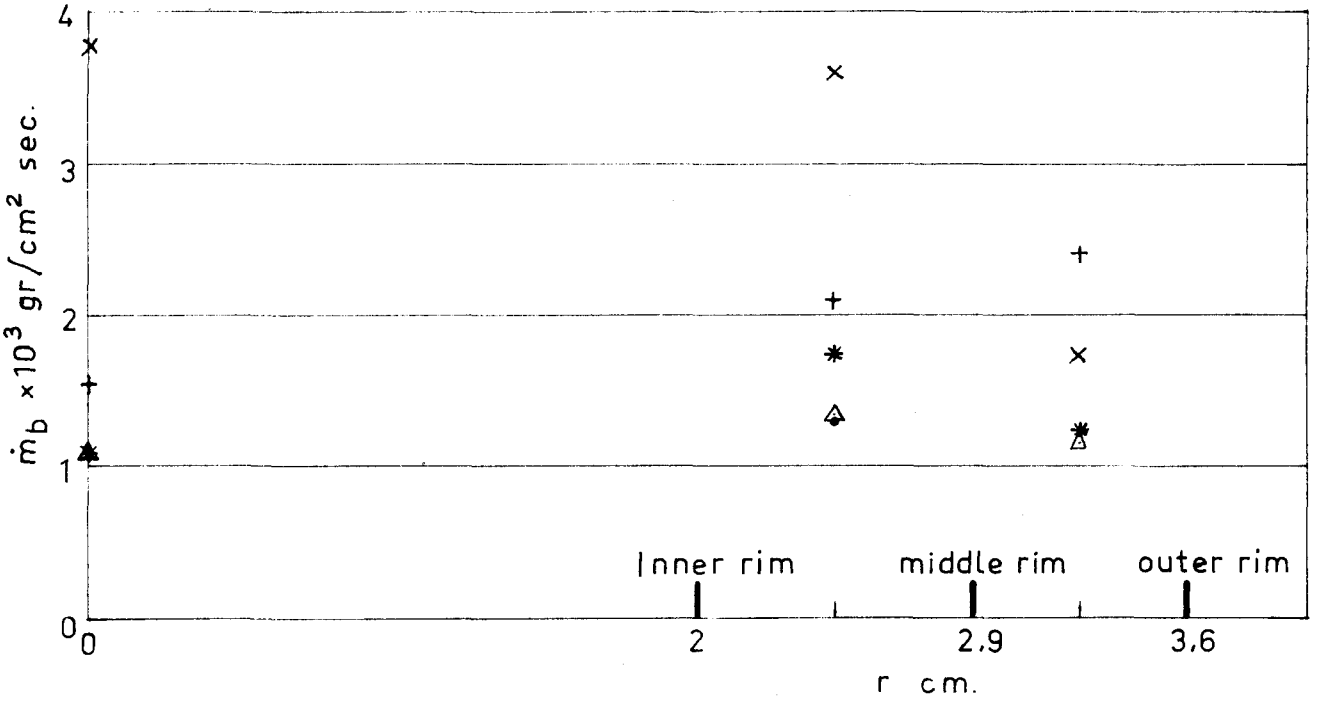

DIOXANE

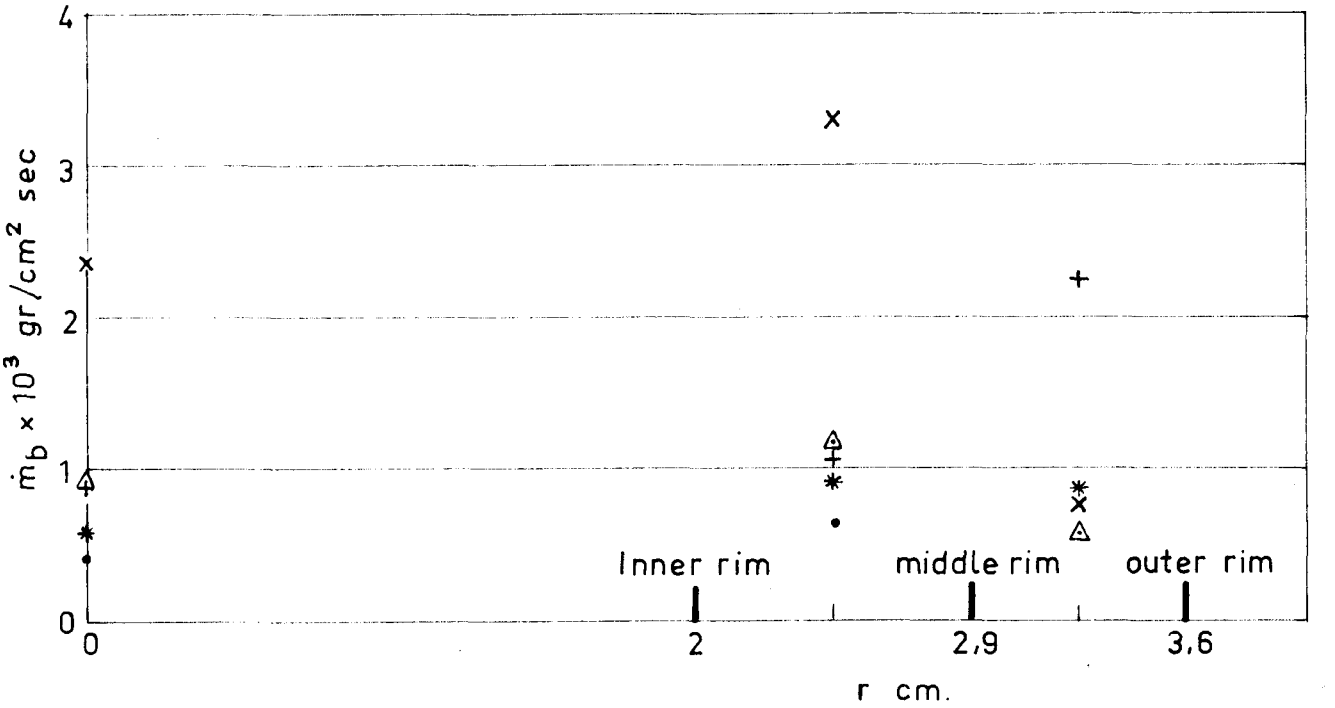

\+ Combustion in all compartments without cooling

* " " " with "

× Combustion in one compartment, other compartments empty

△ " " " " " " with water

• " " central and middle compartments with cooling

EXPERIMENTAL RESULTS

FIG. 9

HEPTANE

Vessel ϕ 250, 205, 144 mm.

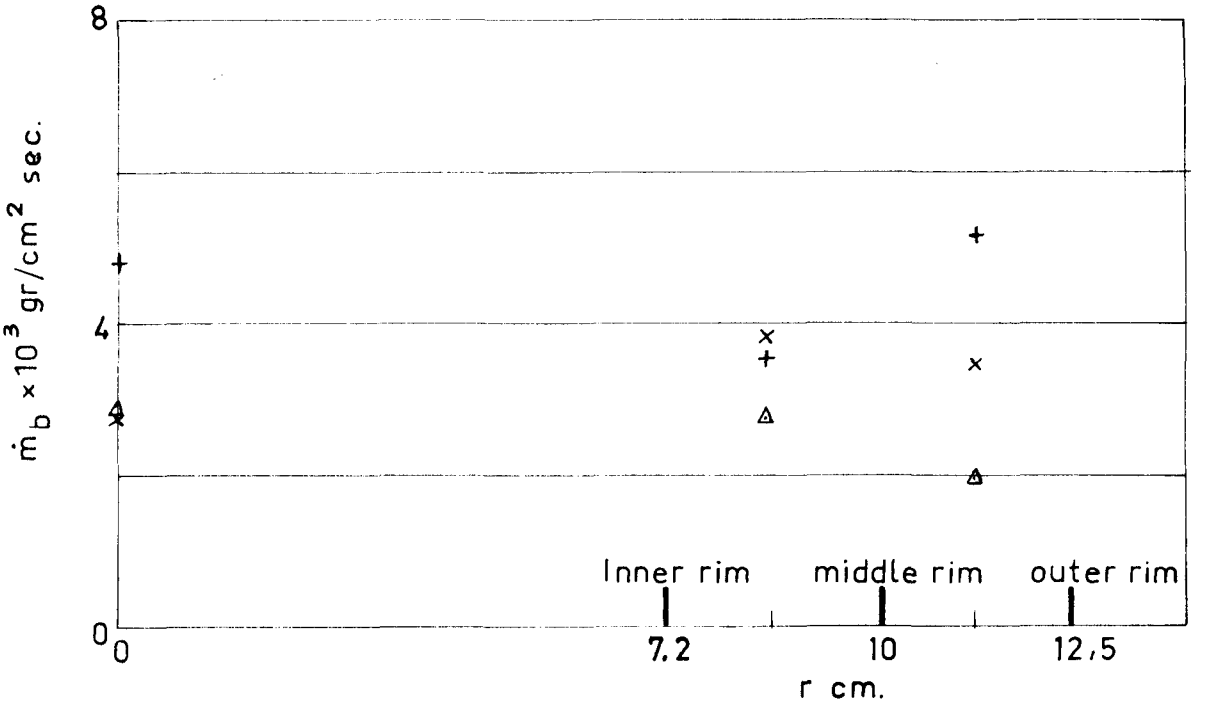

DIOXANE

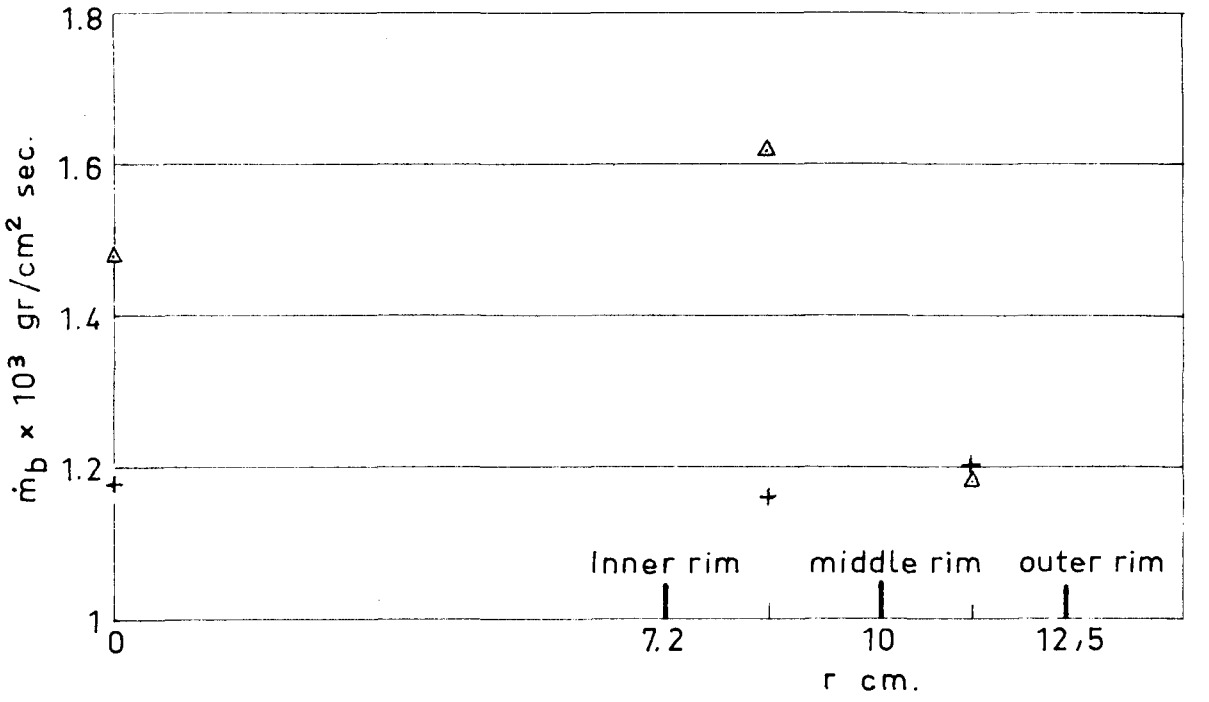

\+ Combustion in all compartments without cooling

× Combustion in one compartment without cooling

△ " " " with "

FIG. 10

VERTICAL FREE-FLIGHT WIND TUNNEL

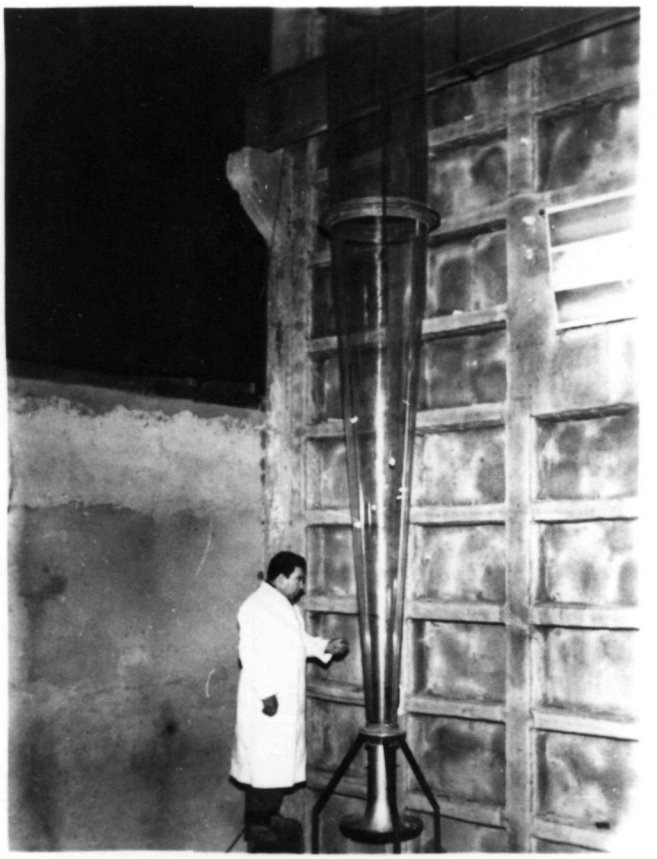

FIG. 11

DIFFERENT TERMINAL VELOCITY V.S. TIME
OAK CYLINDERS

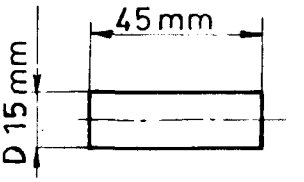

—·—·— Calculated

——— Vertical wind tunnel (firebrands attached)

- - - - - - - - Vertical free-flight combustion tunnel

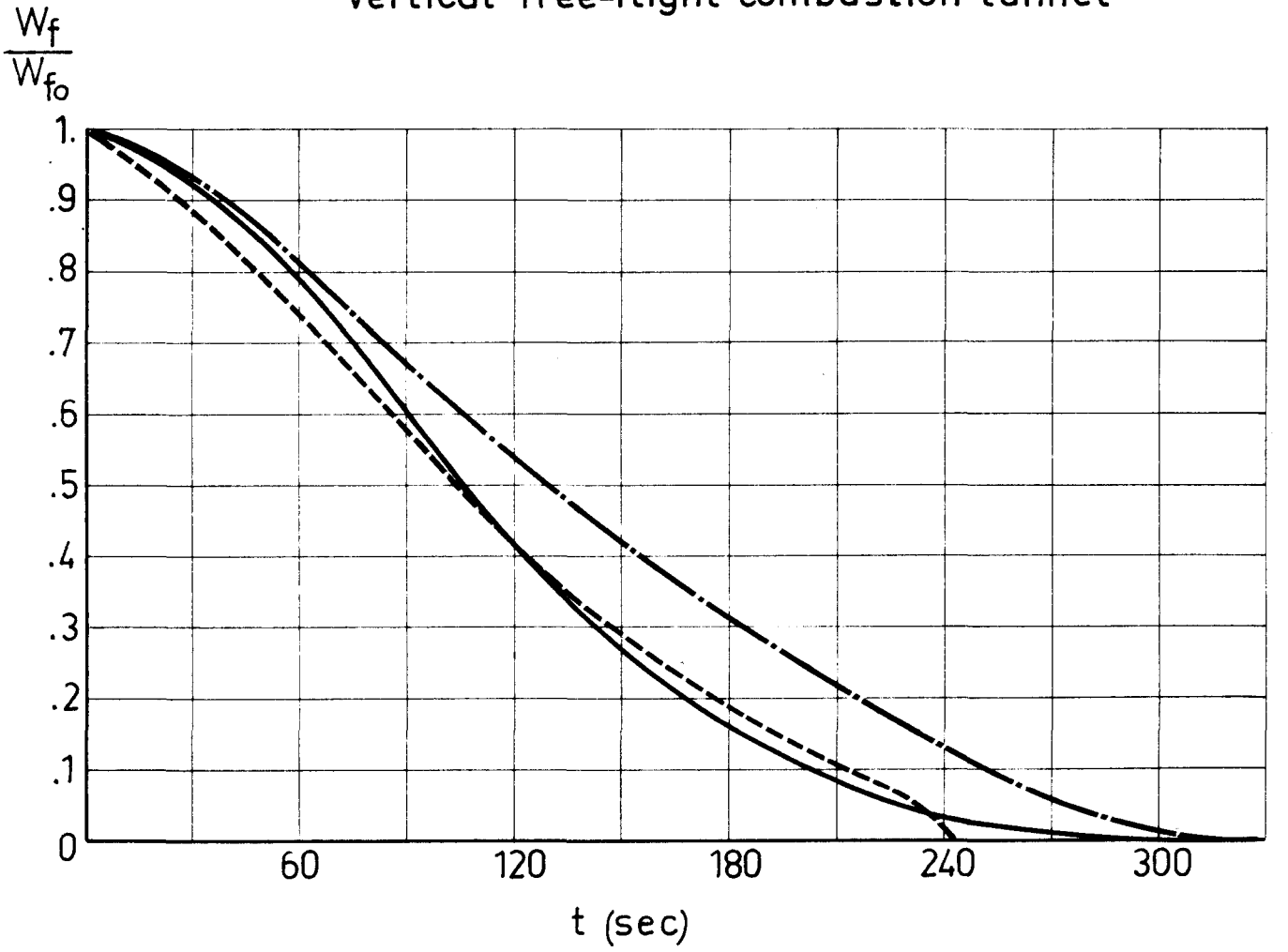

FIG. 12

BURNT-OUT TIME V.S. CHARACTERISTIC RADIUS

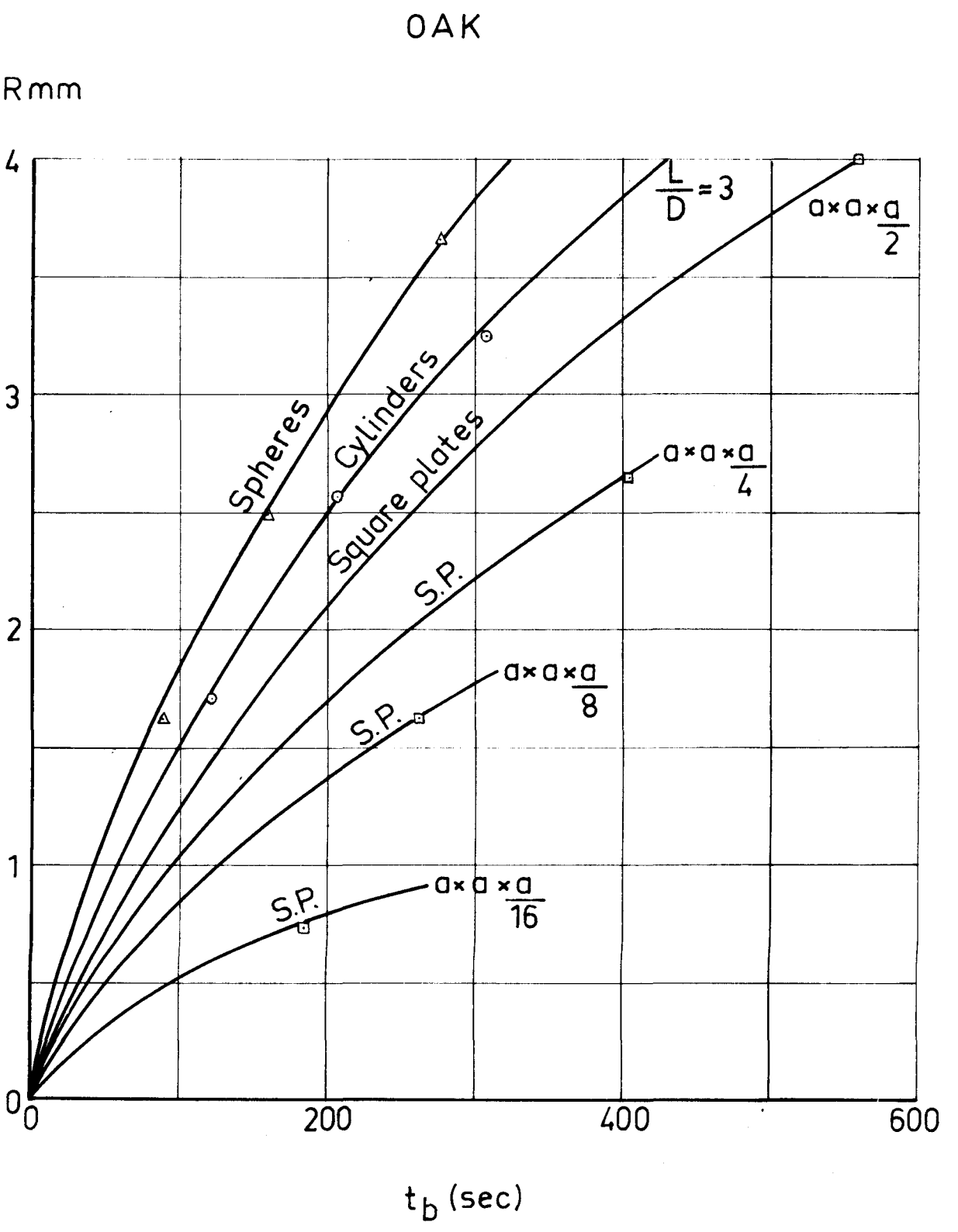

FIG. 13

BURNT-OUT TIME V.S. CHARACTERISTIC RADIUS

PINE

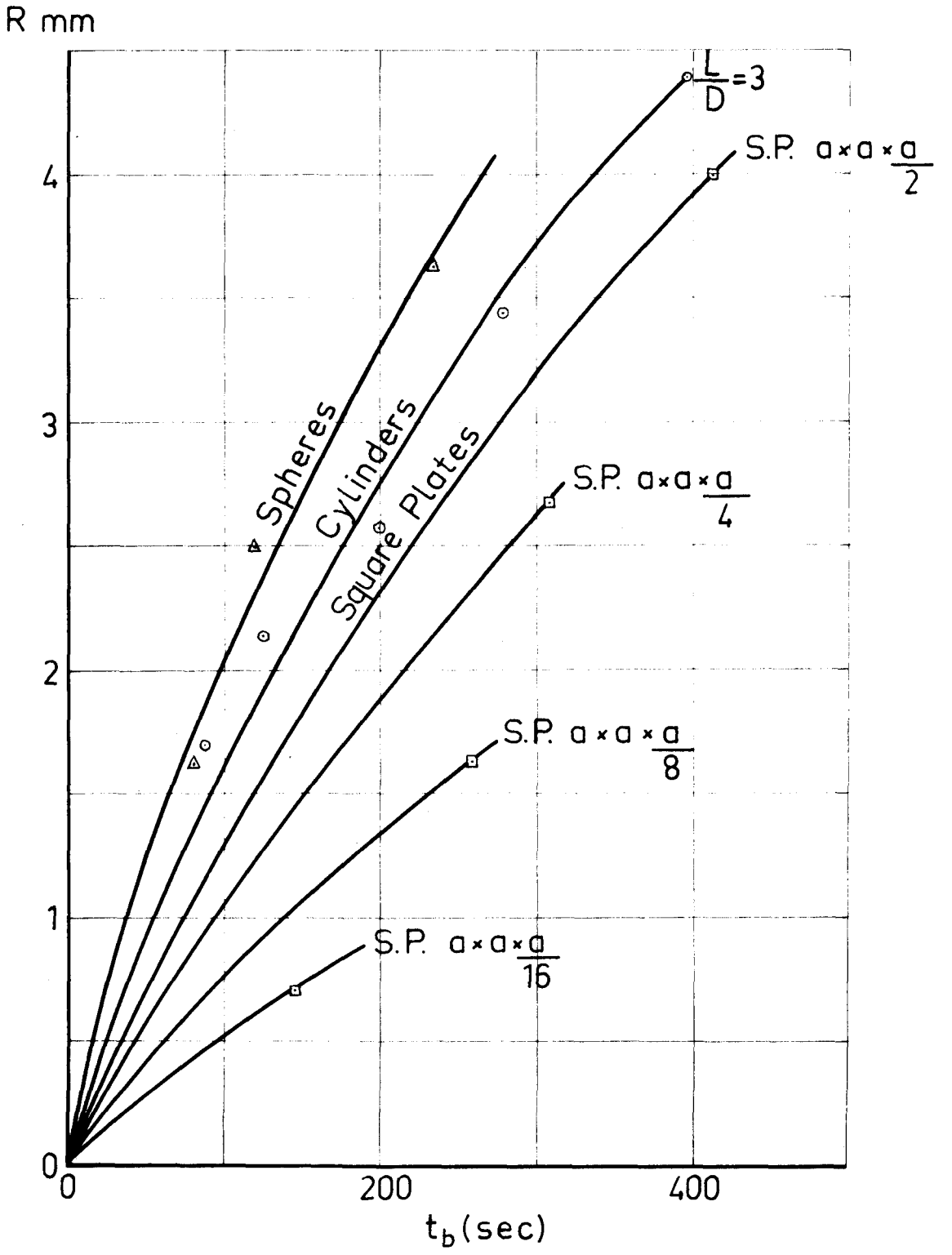

FIG. 14

BURNT-OUT TIME V.S. CHARASTERISTIC RADIUS

ASPEN

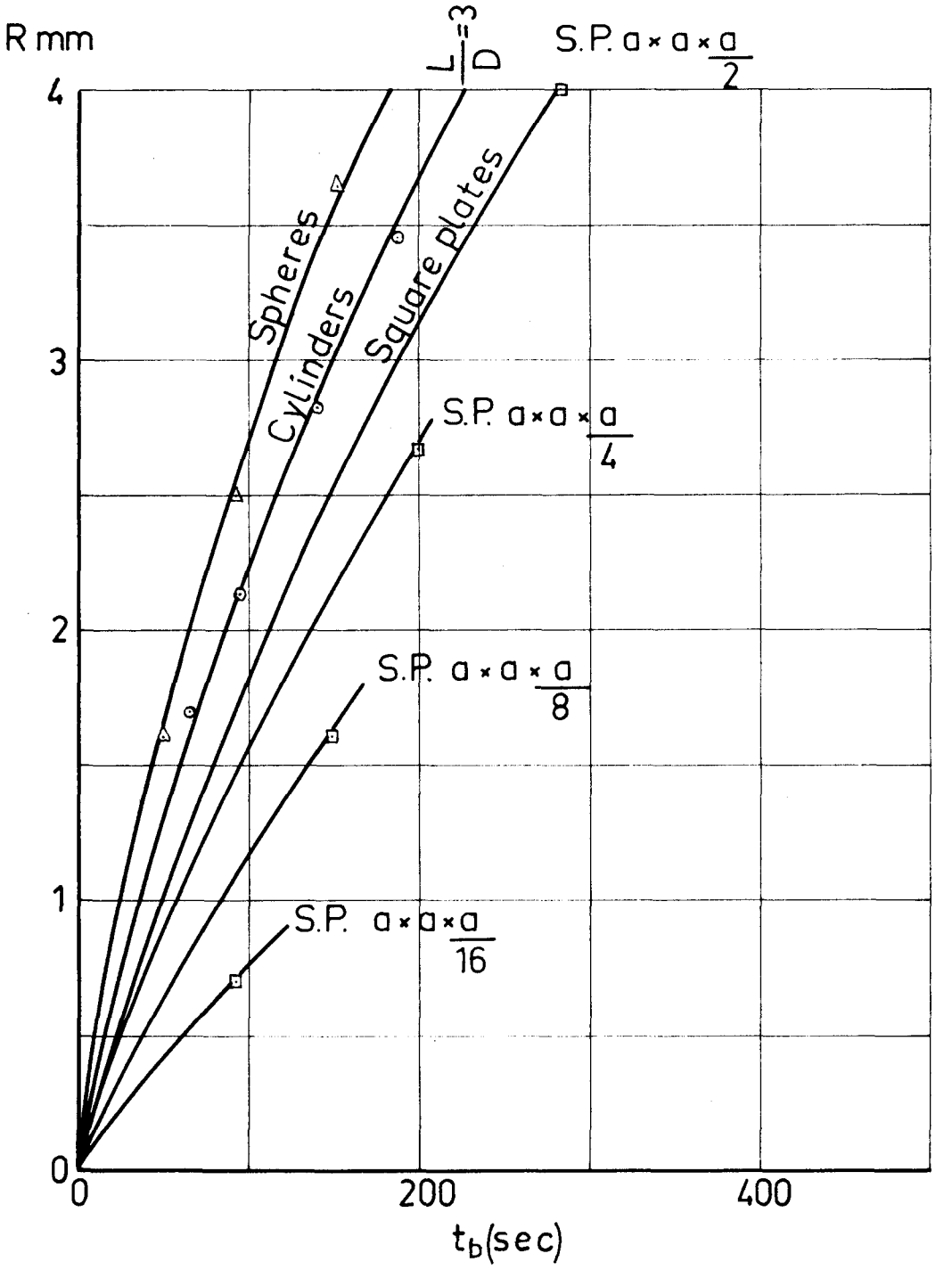

FIG. 15

BURNT-OUT TIME V.S. CHARACTERISTIC RADIUS

BALSA

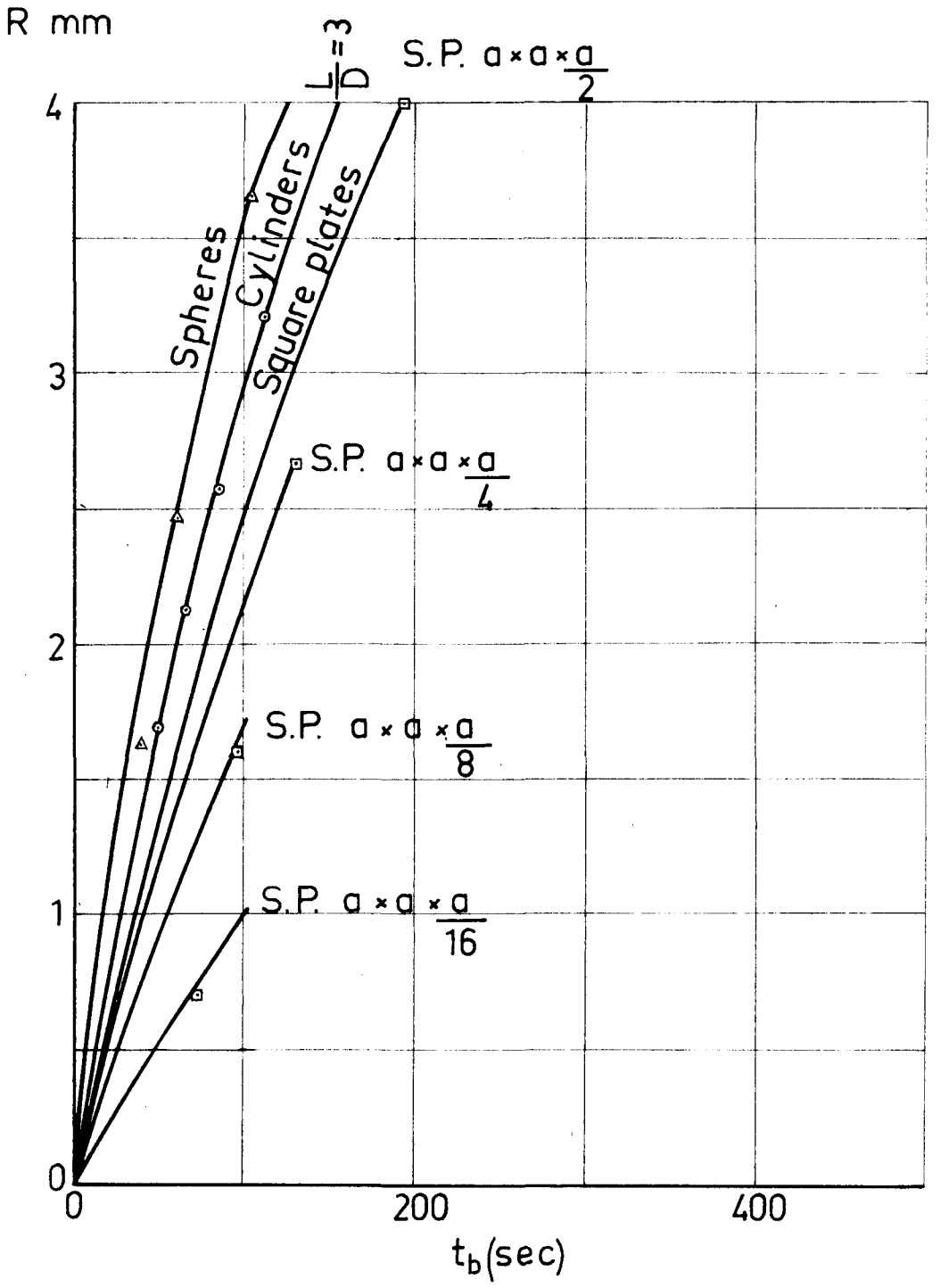

FIG. 16

BURNT-OUT TIME V.S. Re (EQUAL VOLUME SPHERE)

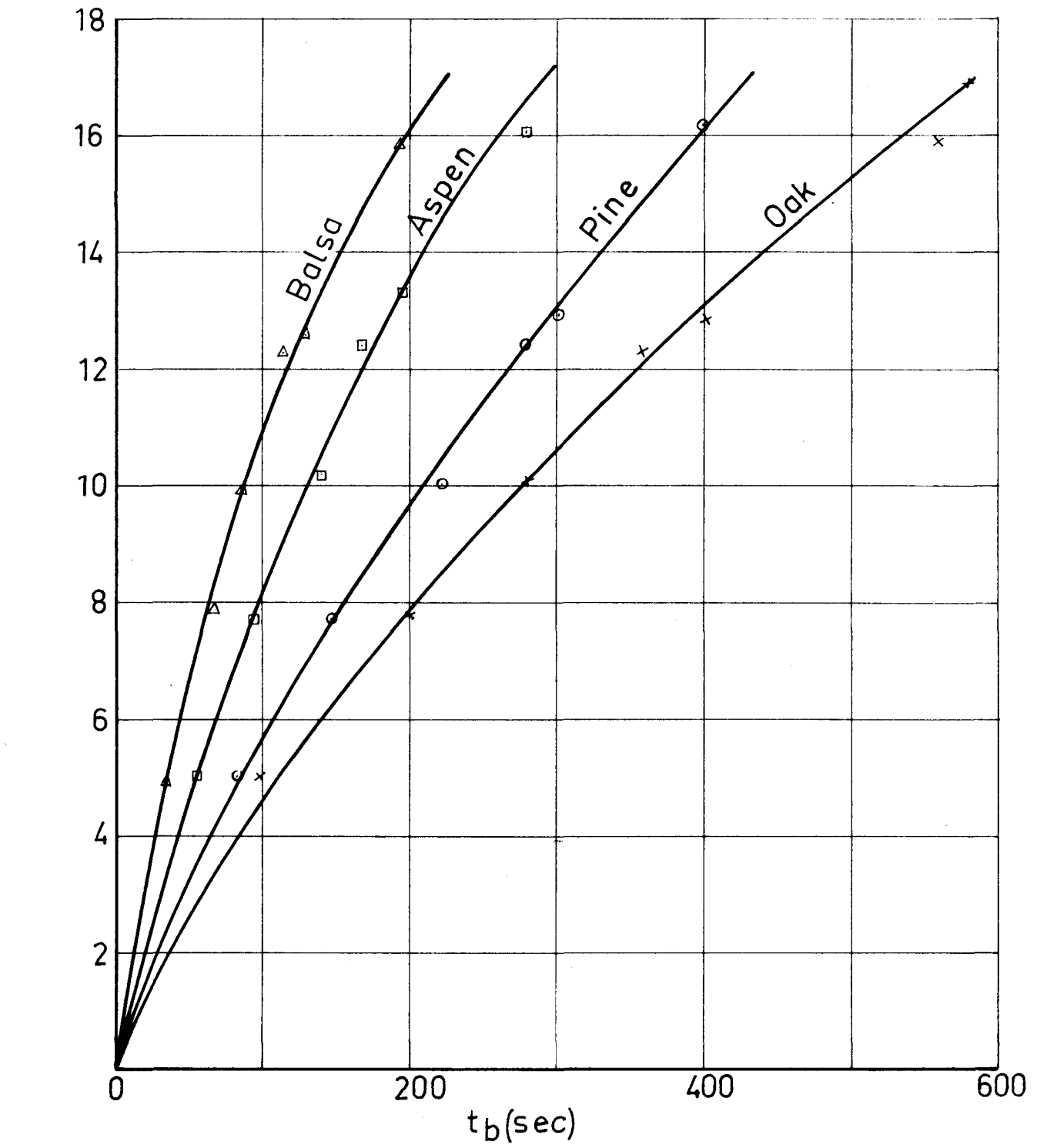

FIG. 17

DIMENSIONLESS WEIGHT V.S. TIME

SPHERES $D_o = 22$ mm.

ASPEN

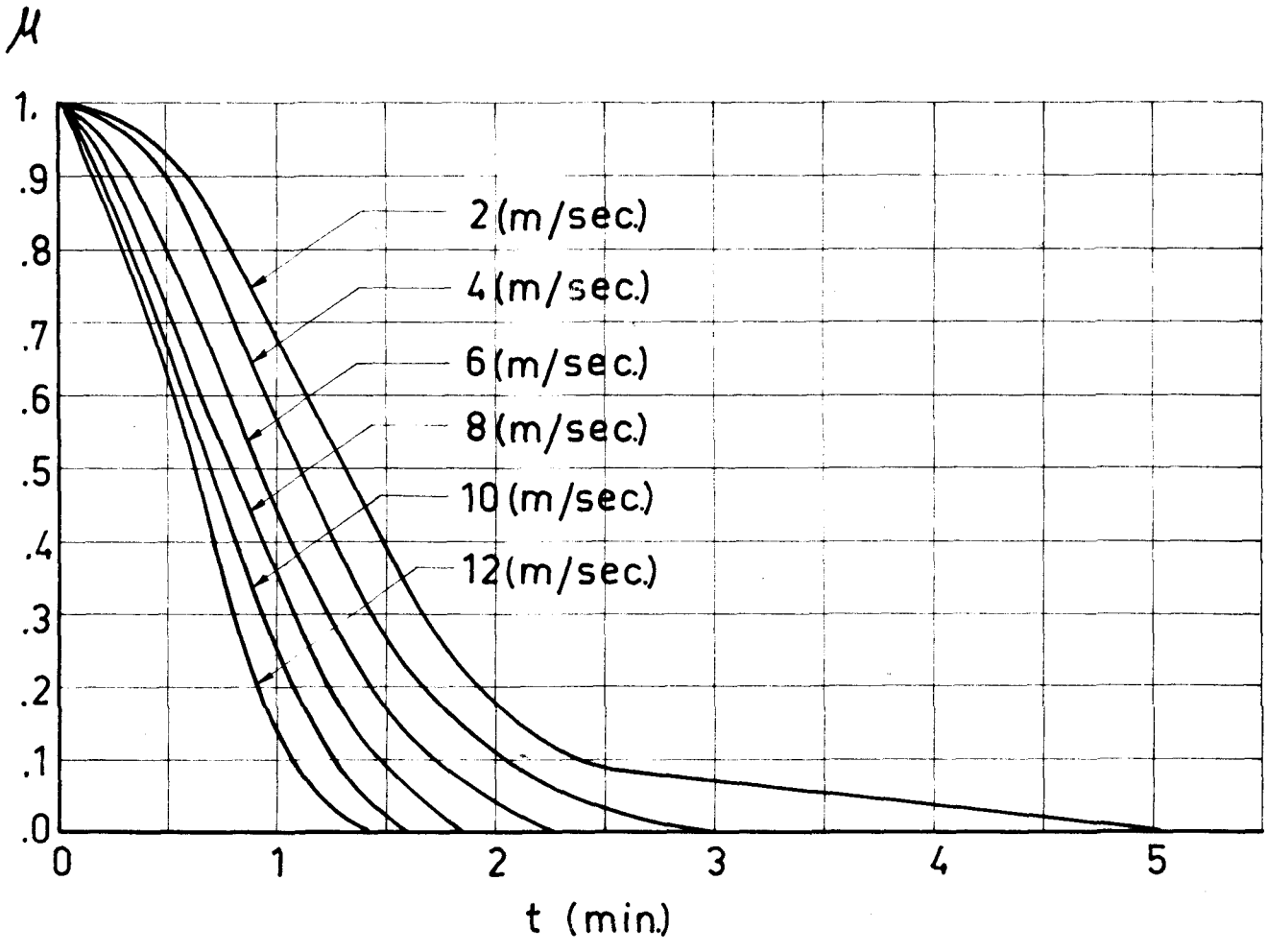

FIG. 18

DIMENSIONLESS WEIGHT V.S.TIME

SPHERES $D_o = 22$ mm.

BALSA

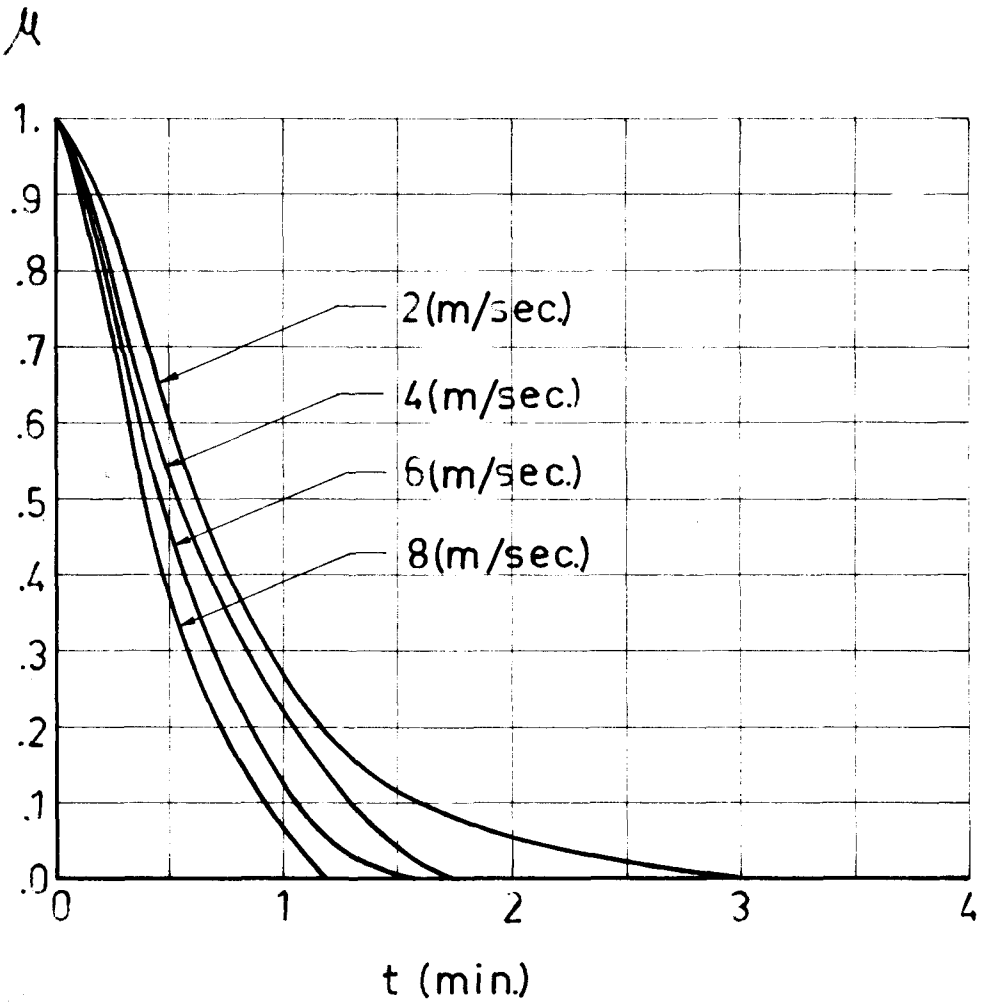

FIG. 19

DIMENSIONLESS WEIGHT V.S. TIME

SPHERES D_o=22 mm.

SPRUCE

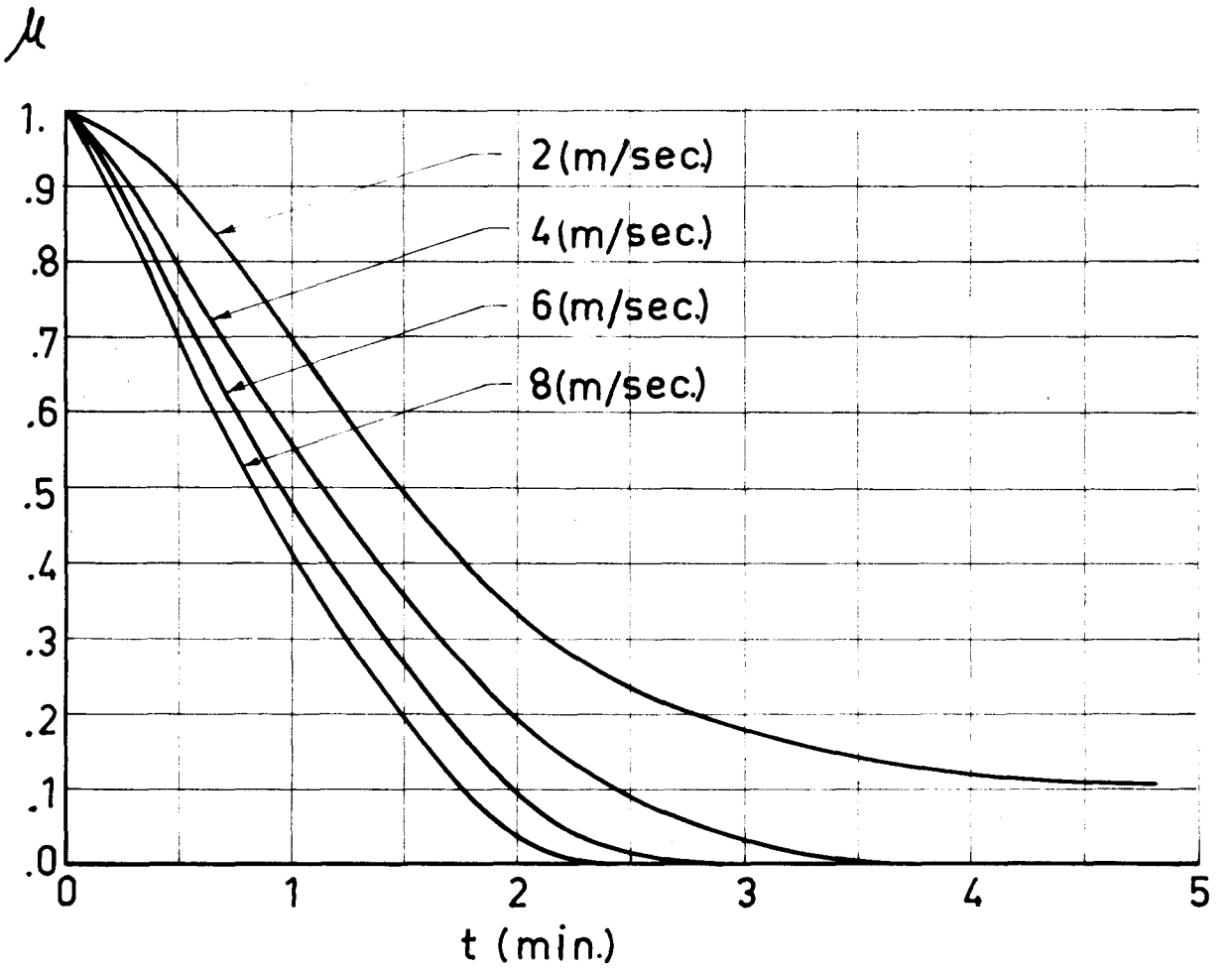

FIG. 20

DIMENSIONLESS VOLUME V.S. TIME

SPHERES $D_o = 22$ mm.

ASPEN

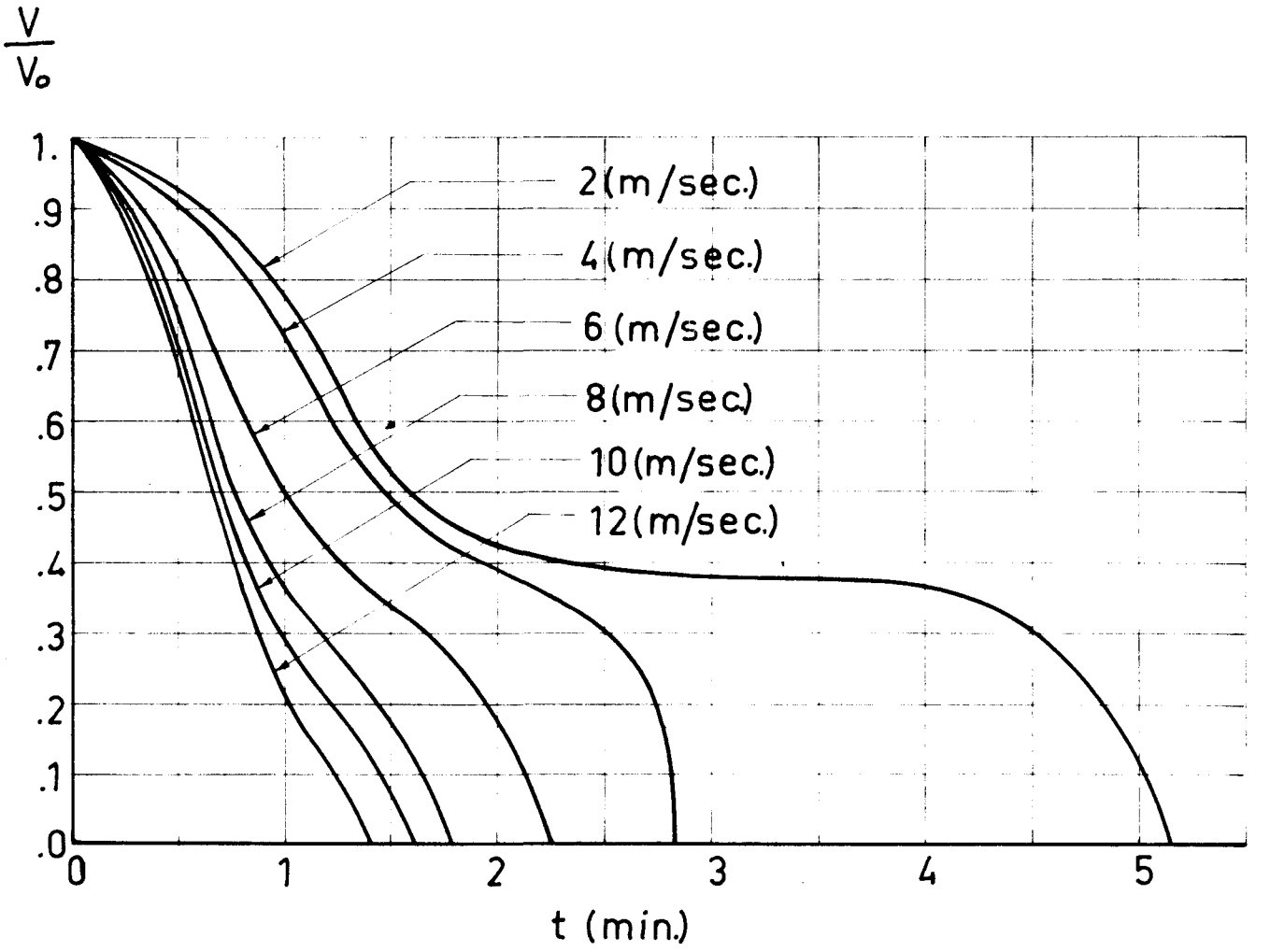

FIG. 21

DIMENSIONLESS VOLUME V. S. TIME

SPHERES D_o = 22 mm.

BALSA

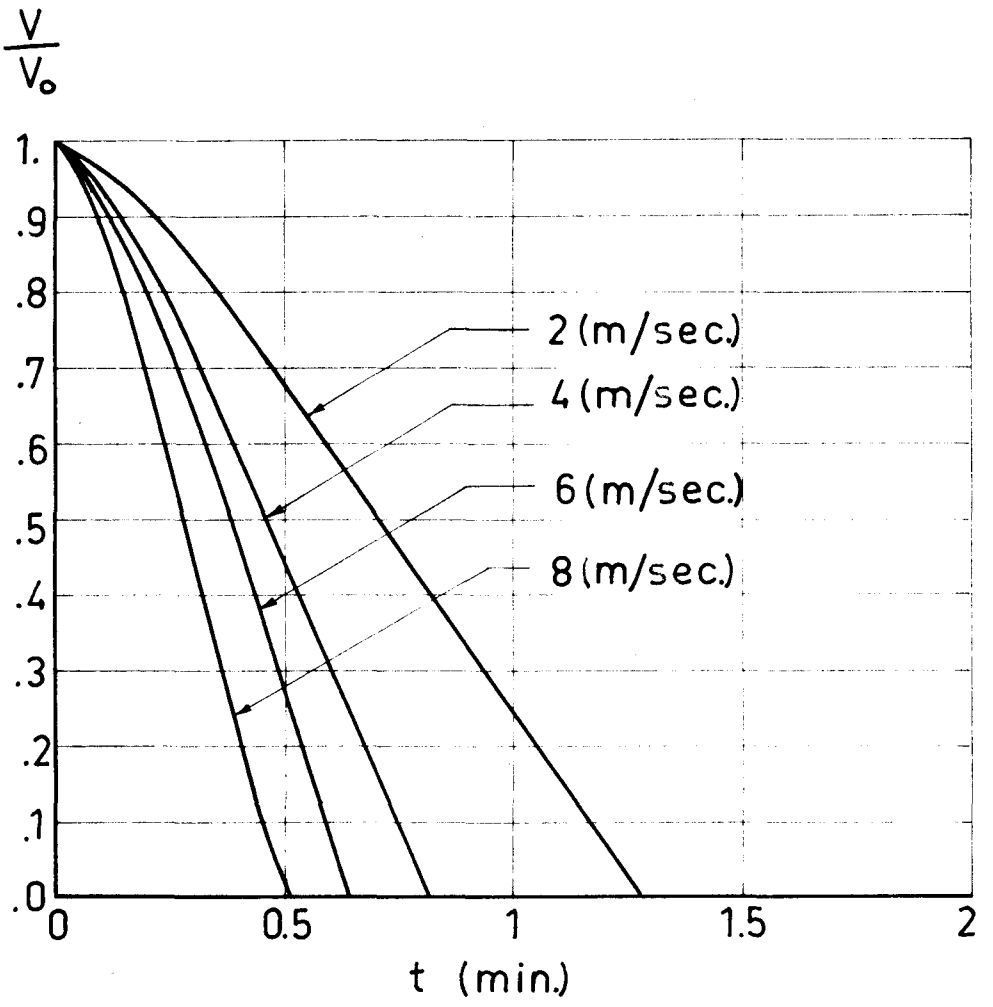

FIG. 22

DIMENSIONLESS VOLUME V.S. TIME

SPHERES $D_o = 22$ mm.

SPRUCE

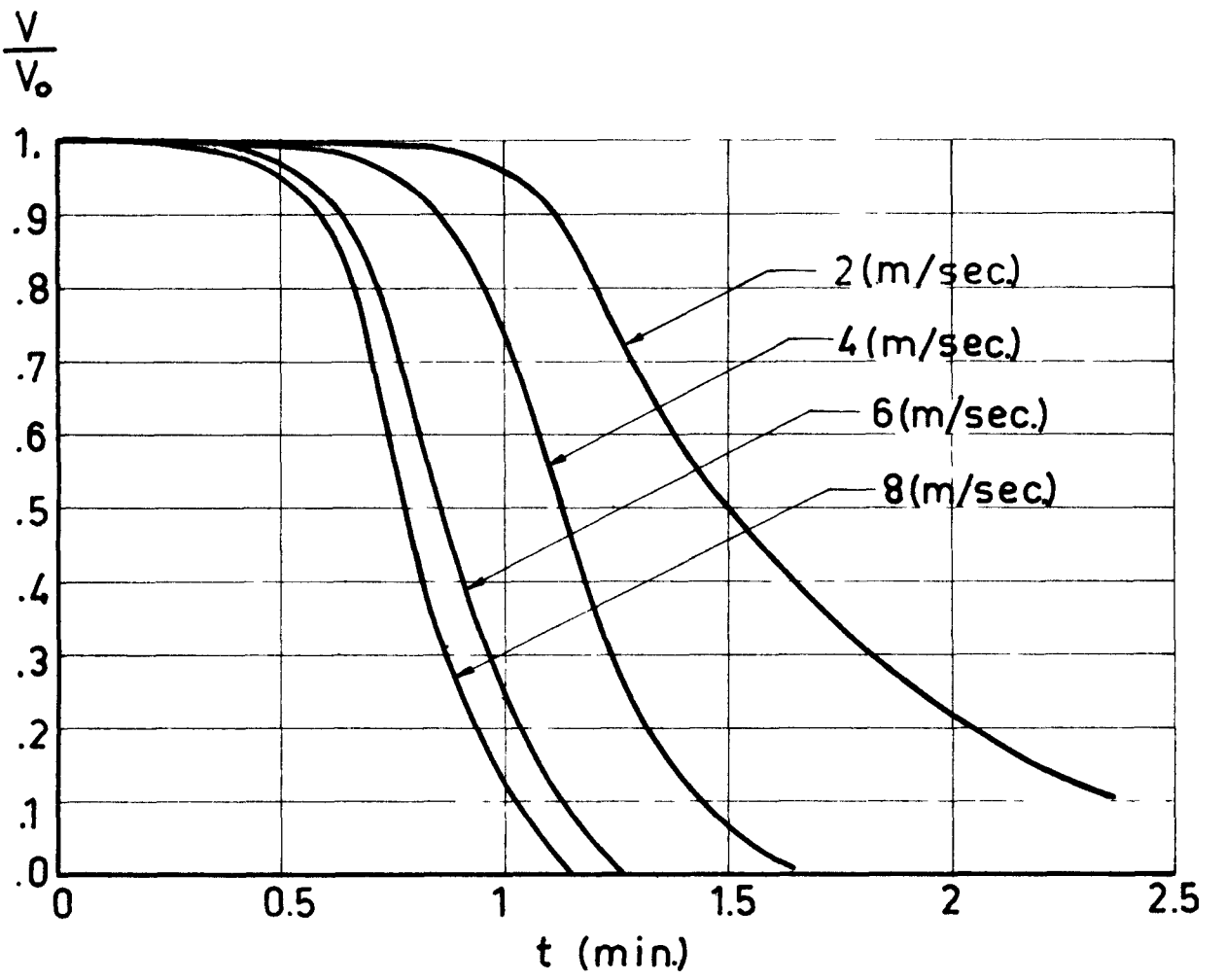

FIG. 23

DIMENSIONLESS EXPERIMENTAL RESULTS
CONSTANT VELOCITY
OAK

SPHERES
- $D_o = 22$ mm.
  - • = 4 (m/sec.)
  - ⊙ = 6 "
  - △ = 8 "
  - × = 10 "
  - ⊡ = 12 "
  - ◈ = 14 "
- $D_o = 15$ mm.
  - ⊕ = 4 (m/sec.)
  - + = 6 "
  - ▲ = 8 "
  - ⊞ = 10 "

CYLINDERS
- $D_o \times L_o =$ 15×45 mm.
  - × = 4 (m/sec)
  - ⊖ = 6 "
  - ■ = 8 "
  - ♦ = 10 "
  - ○ = 12 "
  - ◉ = 14 "
- $D_o \times L_o =$ 12×36 mm.
  - ◇ = 4 (m/sec)
  - ◈ = 6 ("
  - ▣ = 8 "
  - ◈ = 10 "
  - ◈ = 12 "

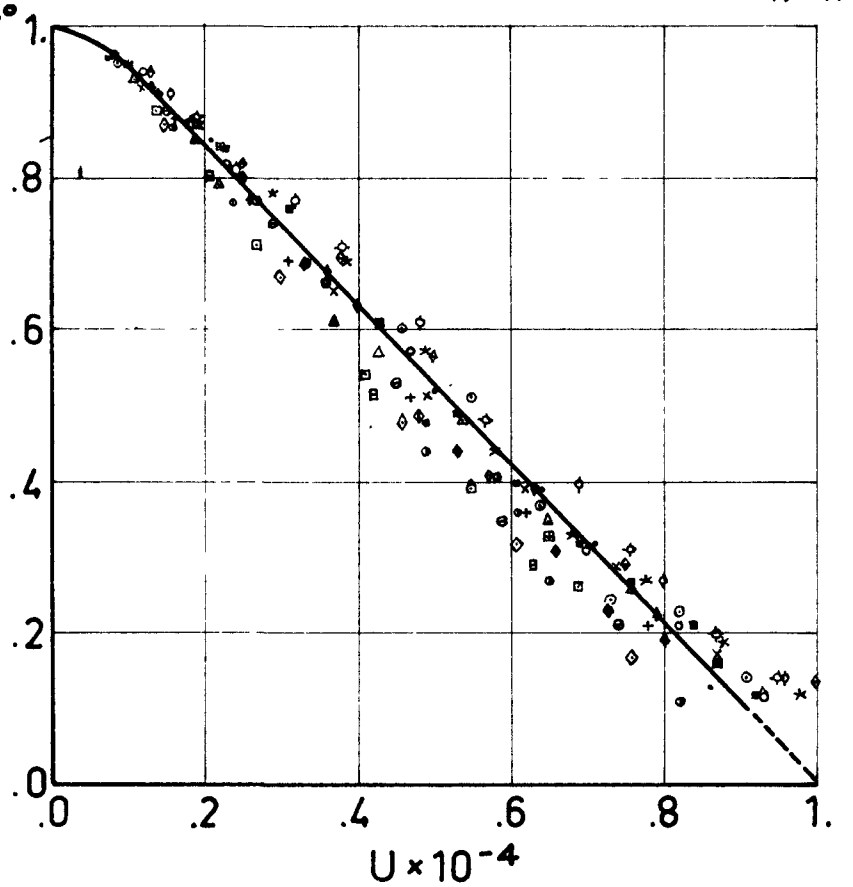

FIG. 24

DIMENSIONLESS EXPERIMENTAL RESULTS
TERMINAL VELOCITY
OAK

CYLINDERS { ⊙ $D_o \times L_o = 15 \times 45$ mm.
△ $D_o \times L_o = 12 \times 36$ mm.

SPHERES { × D_o=22-mm.
◇ D_o=15 mm.

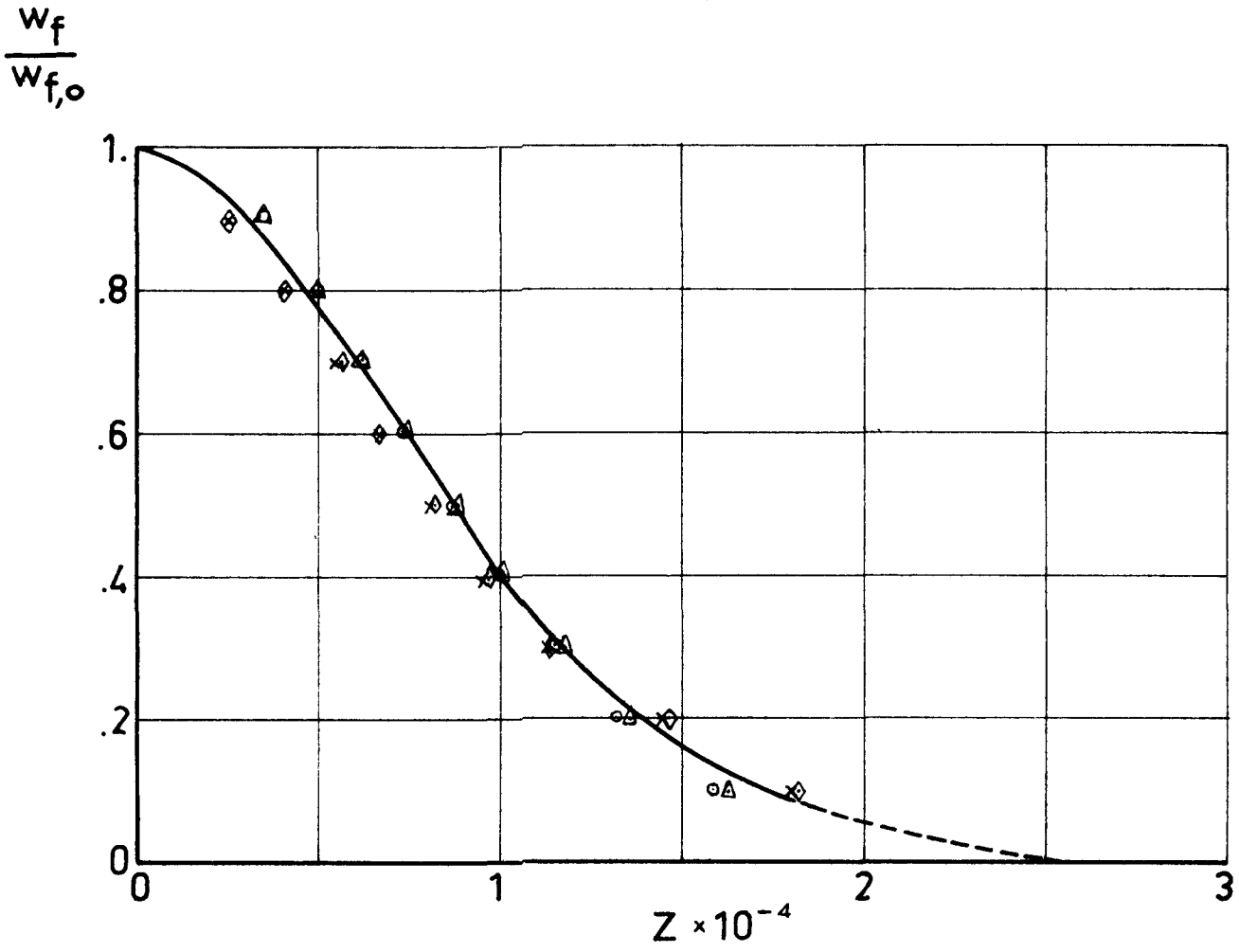

FIG. 25

COMPARISON OF RESULTS

OAK